SAND2018-4566R

US Sections Prepared for Future NEA Crystalline Club (CRC) Report on Status of R&D in CRC Countries Investigating Deep Geologic Disposal in Crystalline Rock

By

P.E. Mariner, E.R. Stein, E.A. Kalinina, T. Hadgu, C. Jove-Colon, and E. Basurto

Sandia National Laboratories is a multi-mission laboratory managed and operated by National Technology and Engineering Solutions of Sandia LLC, a wholly owned subsidiary of Honeywell International Inc. for the U.S. Department of Energy's National Nuclear Security Administration under contract DE-NA0003525.

Table of Contents

1. Introduction 3

2. International collaboration and research activities 3

3. Current concept and state of art of DGR development in the CRC countries 3

4. Characterization of geosphere 8

4.1. Site characteristics 8

4.1.1. Geological Structure 8

4.1.2. Groundwater flow 12

4.1.3. Hydrogeochemistry 17

4.1.4. Solute transport 18

4.1.5. Mechanical and thermal properties 24

4.1.6. Long-term site stability 24

4.2. Laboratory research 24

4.2.1. Sorption properties in fractures engineered barriers, sealing and backfilling measures in crystalline rock mass, of fracture filling material and crystalline rocks 24

4.3. Grouting technology 27

4.4. EDZ 27

5. Safety functions of the geosphere & performance requirements of EBS 29

5.1. Thermal 29

5.2. Hydraulic 29

5.3. Mechanical 29

5.4. Chemical 30

5.5. Seal design, buffer / backfill / seal emplacement, voids filling in a DGR in crystalline rocks 31

6. Safety assessment 32

6.1. Assessment context and system description 32

6.2. FEPs and scenario analysis related to crystalline rocks 33

6.3. Modelling (common words) 34

6.3.1. Modelling of THMC processes in crystalline rock mass and of THMC(B) processes in crystalline rock mass and in EBS 34

6.3.2. Modelling of groundwater flow and radionuclide migration in crystalline rock mass 35

6.3.3. Biosphere transportation models and dose estimation taking into account uncertainty of input data 38

6.4. Uncertainties / confidence in assessment results 40

References (Part 1: Pasted) 41

References (Part 2: From EndNote) 44

1. Introduction

2. International collaboration and research activities

3. Current concept and state of art of DGR development in the CRC countries

3.x United States

3.x.1 Status of U.S. Program

In 2010, the United States (U.S.) began work on a spent nuclear fuel (SNF) program called the Used Fuel Disposition (UFD) campaign. The principal focus of the UFD campaign was to develop options to enable future decision makers to make informed choices about how best to manage SNF and high-level radioactive waste (HLW).

In 2017, the Spent Fuel and Waste Disposition (SFWD) campaign succeeded the UFD campaign, but it continues the primary objectives of the UFD campaign. R&D activities of the campaign include those related to the safety of extended storage, transport, and disposal of SNF and HLW. The U.S. Department of Energy (US DOE) is responsible for permanent disposal of all SNF and HLW in the U.S., and it oversees all related R&D activities.

Disposal R&D has focused on (a) identifying a set of viable geologic disposal alternatives and (b) addressing technical challenges for disposal concepts in various host media (e.g., mined repositories in salt, clay/shale, and crystalline rock) (Gunter and Nair 2016). The goals are to reduce sources of uncertainty that may affect disposal concept viability, increase confidence in the robustness of disposal concepts, and develop the science and engineering tools needed to select, characterize, assess, and license a repository.

US DOE currently has no proposed repository site in crystalline rock nor an operating underground research facility in crystalline rock. To improve its understanding and numerical simulation of crystalline rock, US DOE and its contractors conduct basic laboratory research, develop repository concepts for crystalline rock, and develop computational tools for simulating the flow and transport of heat, fluid, and radionuclides through crystalline rock. Through international projects, US DOE collaborates in data exchanges and joint experiments at sites and underground facilities around the world. Crystalline repository programs in Europe, North America, and Asia have generated valuable data from laboratory and field experiments and have produced refinements to repository design concepts. Active collaboration with international experts is beneficial to US DOE because data and information shared in these programs increase US DOE's knowledge base and modelling capabilities.

U.S. expertise in crystalline rock has advanced over the past several years largely owing to international collaborations. The U.S. is an active member in the DECOVALEX (DEvelopment of COupled models and their VALidation against EXperiments) Project which is an international research collaboration activity for advancing the understanding and mathematical modeling of coupled thermo-hydro-mechanical (THM) and thermo-hydro-chemical (THC) processes in geological systems. The U.S. participates or has participated in data exchanges and tests at several international underground research facilities including the Grimsel Test Site in Switzerland, the KAERI (Korea Atomic Energy Research Institute) underground research tunnel (KURT) in the Republic of Korea, and the Mizunami underground research facility in Japan. Several U.S. activities at underground research facilities related to disposal in crystalline host rock are discussed later in different sections of this report.

U.S. knowledge in deep geologic disposal in crystalline rock is advanced and growing. U.S. status and recent advances related to crystalline rock are discussed throughout this report. Brief discussions of the history of U.S. disposal R&D and the accumulating U.S. waste inventory are presented in Sections 3.x.2 and 3.x.3. The U.S. repository concept for crystalline rock is presented in Section 3.x.4. In Chapters 4 and 5, relevant U.S. research related to site characterization and repository safety functions are discussed. U.S. capabilities for modelling fractured crystalline rock and performing probabilistic total system performance assessments are presented in Chapter 6.

3.x.2 Brief History of U.S. Disposal R&D

U.S. research in underground disposal of radioactive waste began in the 1950s with a focus on deep salt formations. By the late 1970s and early 1980s, research expanded to crystalline rock. The U.S. developed an underground research laboratory (URL) at a depth of 420 m in the Climax monzonite stock, a granitic body at the Nevada Test Site (Figure 1). Work at this URL demonstrated the feasibility and safety of SNF storage and retrieval from a facility in granite (Patrick 1986).

The enactment of the Nuclear Waste Policy Amendments Act of 1987 cut nearly all U.S. research on crystalline rock for two decades. This act directed US DOE to focus exclusively on the Yucca Mountain site (welded tuff) in Nevada and phase out funding for research in other host rocks. The funding phase out, however, did not prevent development in the early 1990s of a probability-based PA model for disposal of DOE-managed SNF in granite (SNL 1993). The results of that model indicate that, with adequate treatment and packaging, all waste forms considered could be isolated from the environment with acceptable performance for 10,000 years.

By 2008, US DOE built and documented a complete safety case for the Yucca Mountain repository and had submitted a license application. Two years later, Congress suspended funding for the project. At that point, the UFD campaign was initiated (Section 3.x.1), and the development of new US repository concepts, including a concept for crystalline rock (Mariner et al. 2011), was underway.

Figure 1. Waste disposal demonstration in granite at the Nevada Test Site (Patrick 1986).

3.x.3 U.S. Inventory

As of 2017, there were over 77,000 metric tons of heavy metal (MTHM) of commercial SNF in temporary storage at 75 reactor sites in 33 states across the U.S. (Bonano et al. 2018). Most of this SNF is stored in pools with the remainder in dry storage. Currently, about 160 new dry storage canisters are loaded each year. Because pool storage has reached capacity, dry storage is projected to surpass pool storage by 2028. Assuming full license renewals and no new reactor construction, the total volume of commercial SNF in 2048 is projected to be approximately 184,000 m^3 (140,000 MTHM).

In addition to commercial SNF, US DOE-managed SNF and HLW also await disposal. Approximately 2,500 MTHM of US DOE-managed SNF and 20,000 canisters of HLW are temporarily stored at several facilities across the U.S. (Marcinowski 2010; Bonano et al. 2018). The amounts of these materials are much lower than that of commercial SNF. In 2048, the total volumes of HLW and US DOE SNF are projected to be around 26,000 m^3 and 7,000 m^3, respectively.

3.x.4 U.S. Repository Concept

The primary purpose of a deep geologic repository is to provide an acceptably low probability of an unacceptable level of radionuclide release to the biosphere. The repository concept is a set of engineered and natural barriers that work together to achieve this purpose.

The U.S. repository concept for a crystalline rock repository is schematically illustrated in Figure 2. The system consists of several engineered and natural barriers: waste forms, waste packages, buffer/backfill, seals/liners, disturbed rock zone (DRZ), host rock, and biosphere. In the near- and far-fields, which extend from the EBS buffer through the geosphere, a complex set of coupled physical and chemical processes control radionuclide release. Within the EBS, the processes include radionuclide decay and ingrowth, waste package degradation, instantaneous radionuclide release, waste form dissolution, buffer degradation, chemical interactions (mineral precipitation and dissolution, sorption, cation exchange), thermal effects (advection, conduction), fluid flow by advection and diffusion, and mechanical processes. Important processes considered within the geosphere include radionuclide decay and ingrowth, groundwater flow in fractures and the DRZ, advective transport and longitudinal dispersion of radionuclides within fractures, mixing at fracture intersections, radionuclide retention by diffusion into rock matrix, and sorption on matrix mineral grains.

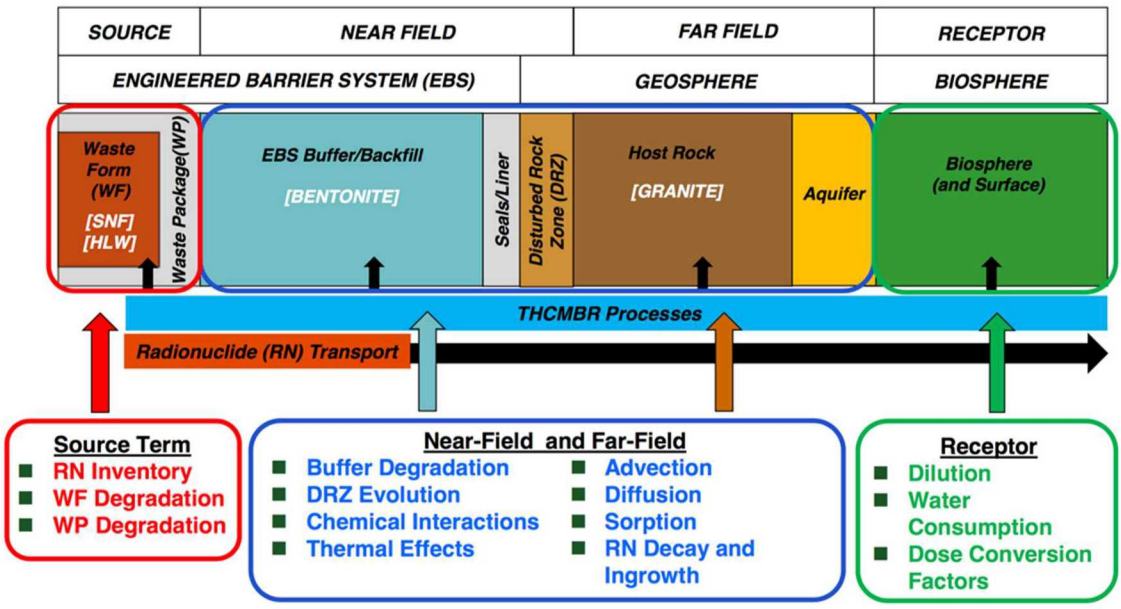

Figure 2. Multiple-barrier concept for a repository in crystalline rock (Wang et al. 2014)

Repository Layout

Based on the general concept in Figure 2, a reference repository design was developed (Wang et al. 2014). A site-scale illustration of the general design is shown in Figure 3. The reference design is intended to provide generic specifications for the repository system, with the purpose of using it to construct a total system performance assessment (TSPA) model.

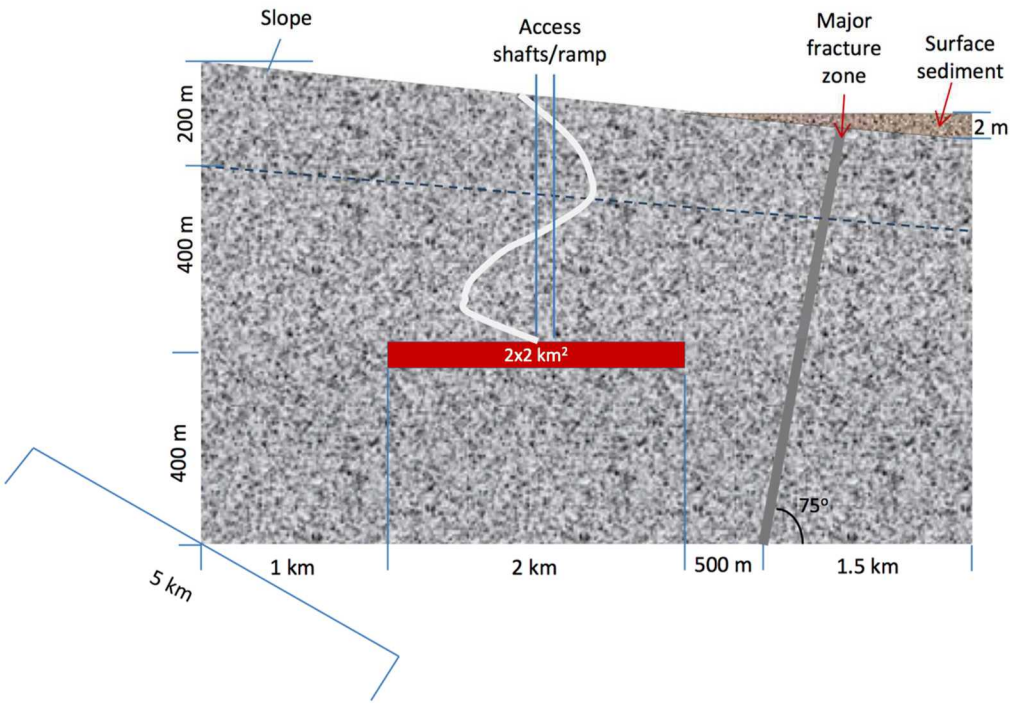

Figure 3. Illustration of the general U.S. repository concept for crystalline host rock (Wang et al. 2014)

Consistent with the reference cases developed for other potential host rock (Freeze et al., 2013; Jove-Colon et al., 2014), several assumptions were adopted for the crystalline repository reference case:

- The repository is excavated at a depth of about 600 meters within a water-saturated igneous intrusion or metamorphic rock.
- The horizontal repository layout consists of excavated emplacement drifts separated by the host rock, and connected by a horizontal operation tunnel that can be accessed by both an access ramp and vertical shafts. The access ramp facilitates the transportation of large waste packages.
- The repository has a waste disposal capacity of 70,000 MTHM.
- Waste packages (canister/container plus disposal overpack) are permanently sealed to avoid any risk of additional exposure during handling operations. For disposal, each waste package is encapsulated by multi-layered buffer materials.
- The repository is able to accommodate waste packages of various sizes. Waste packages are emplaced in vertical boreholes on the drift floor or directly in the drifts (especially for dual purpose canisters due to their large sizes). Disposal drifts are backfilled with a mixture of clay material and crushed crystalline rocks. Multi-layered backfilling is part of the EBS configuration.
- The thermal limit of the buffer/backfill materials is assumed to be 200°C. No thermal limit is assumed for the crystalline host rocks.

- The access ramp and shafts are used for construction, waste handling/emplacement operations, and ventilation. Drifts and access/operation shafts are sealed at closure.
- The waste is retrievable for a period of 50 years after waste emplacement operations are initiated.

The repository is intended to include distinct types of waste packages, which are expected to be emplaced in different areas of the repository with varying waste package spacing and drift spacing (Wang et al. 2014). Layout dimensions for 12-PWR waste packages includes a waste package (end-to-end) spacing of 5 m and drift spacing of 20 m. Dual-purpose canisters (DPCs), i.e., canisters that can also be loaded into licensed transportation casks, are much larger than 12-PWR waste packages and require a different layout. For DPCs, the waste package spacing is 10 m and drift spacing of 70 m. Drift and package spacing is dictated by the maximum temperature allowed in the buffer. Liu et al. (2013) provides a summary of the thermal constraints on EBS bentonite imposed in disposal concepts throughout the world for disposal in argillite and crystalline host-rock media. A conservative thermal limit of 100°C is used in each of these disposal concepts regardless of differences in EBS design concepts.

Waste inventory

The assumed capacity for the developed repository concept is 70,000 MTHM. For simplicity, the entire waste inventory in the reference repository concept is assumed to be comprised of pressurized water reactor (PWR) SNF assemblies. This inventory can be expanded to include boiling water reactor (BWR) and HLW inventories as the reference design is further developed. The reference case PWR SNF inventory consists of about 450 isotopes (Carter et al. 2013).

Engineered Barrier System

The EBS components of the crystalline repository concept include the following:

- Two types of waste packages: DPCs and 12-PWR waste packages. The DPCs are assumed to contain 32 PWR SNF assemblies, although many DPCs are now being loaded with 37 assemblies and many older DPCs have fewer. A 12-PWR waste package is composed of a stainless-steel canister/container in addition to an enclosing disposal overpack. Materials for disposal overpack can range from stainless steel, copper, and carbon steel depending on the barrier operational design (e.g., corrosion allowance) within the EBS concept. The base case concept is for stainless steel waste packages and carbon steel DPC overpacks.
- Bentonite buffer/backfill: An engineered clay buffer backfill is emplaced in a multi-layered configuration to optimize thermal, flow, and sorption properties of the buffer/backfill media. FEBEX and MX-80 are two bentonites that are being considered for use due to their thermal, hydrological and mechanical properties.
- Seals/liners: Seals and liners made of cement and clay material are used in the access shafts and on the walls of the repository to limit radionuclide transport and fluid flow beyond the repository.

Natural Barrier System

The primary natural barrier in the repository concept is the crystalline host rock. The concept for a mined repository in crystalline rock positions the repository 600 m below the land surface in a sparsely fractured crystalline rock that either outcrops or subcrops near the surface (Mariner et al. 2016). Regionally, the topographic slope is less than 1°, and the water table is unconfined, a combination which delivers little driving force for deep fluid flow. The reference repository is located in a stable cratonic terrain with low probabilities of seismicity, igneous activity, and human intrusion. Low probability for human intrusion is reduced by avoiding regions with known geologic resources such as extensive fresh water aquifers, ore deposits, fossil fuels, or high geothermal heat flux. This concept is consistent with international concepts of disposal in crystalline rock (e.g., SKB 2007).

Crystalline Host Rock

The representation of fractured crystalline host rock in recent generic simulations of the repository concept (e.g., Mariner et al. 2016; Stein et al. 2017) is primarily based on the well-characterized, sparsely fractured metagranite at Forsmark, Sweden (Follin et al. 2014; Joyce et al. 2014). The Forsmark site sits in the Fennoscandian Shield and consists of crystalline bedrock (primarily granite with lesser amounts of granodiorite, tonalite, and amphibolite) that formed between 1.89 and 1.85 Ga (1 Ga = 1 billion years), experienced ductile deformation and metamorphism, and cooled to the limit of brittle deformation between 1.8 and 1.7 Ga (SKB 2007). Subsequent

brittle deformation occurred associated with later tectonic events (1.7 to 1.6 Ga and 1.1 to 0.9 Ga), and recent glaciation (< 1 Ma) has resulted in crystalline basement outcrops and thin (<25 m) Quaternary sedimentary deposits of variable thickness and extent (SKB 2008). Crystalline basement with similar history exists within the United States (for instance at the southern margin of the approximately 2-Ga-old Superior Craton in Minnesota and Wisconsin (e.g., Stone et al. 1989), and can be reasonably expected to have similar hydraulic properties.

The migration of fluid and radionuclides through the crystalline host rock is conceptualized as flow and diffusion through fractures and matrix. Numerically it is simulated using two types of grid cells: those containing a fracture or fractures and those without fractures (the matrix). Hydraulic parameters (permeability and porosity) describing fractured cells are derived from fracture parameters developed for the Forsmark metagranite (Follin et al. 2014; Joyce et al. 2014; Wang et al. 2014). Parameters describing matrix cells are derived from measurements made in tunnel walls of underground research laboratories in crystalline rock at the Grimsel Test Site, Switzerland (Schild et al. 2001; Soler et al. 2015), Lac du Bonnet batholith, Canada (Martino and Chandler 2004), and the Korean Underground Research Tunnel (Cho et al. 2013). All other parameters are identical in fracture and matrix cells.

Performance assessment simulations to date tend to have a conservative bias toward fracture connectivity (Stein et al. 2017). Connectivity is required to create a percolating network. Nevertheless, simulations of multiple fracture realizations run to 1 million years indicate that, because of the channelled nature of fracture flow, thermally-driven fluid fluxes associated with peak repository temperatures may be a primary means of radionuclide transport out of the repository. Selected simulations are described in Chapter 6.

4. Characterization of geosphere

4.1. Site characteristics

4.1.1. Geological Structure

4.1.1.x USA

4.1.1.x.1 Fracture Mapping at Mizunami Underground Research Laboratory

Understanding subsurface fracture network properties at the field scale is important for a number of environmental and economic problems, including siting of spent nuclear fuel repositories, geothermal exploration, and many others. This typically encompasses large volumes of fractured rocks with the properties inferred from the observations at rock outcrops and, if available, from the measurements in exploratory boreholes, quarries, and tunnels. These data are inherently spatially limited and a stochastic model is required to extrapolate the fracture properties over the large volumes of rocks. An approach to developing a discrete fracture model using the data collected at the Mizunami Underground Research Laboratory (MIU) is described below. The details are provided in Kalinina et al. (2018).

A discrete fracture network (DFN) model was developed for the area surrounding the MIU Research tunnel at 500 m depth using FRACMAN (Golder Associates, Inc., 2017). The modelling domain is 100 x 150 x 100m with the main experimental part of the tunnel, Closure Test Drift (CTD), located approximately in the center. The following data were used in the fracture analysis:

- Fracture traces on the walls of CTD, Inclined Drift, and Access Drift.
- Fractures observed in borehole 12MI33.
- Packer test data in 6 test intervals of 12MI33.
- Measured inflow into the research drift.

Two thousand and twenty-three fractures were observed on the wall of the research tunnel. It was assumed that the fractures that did not exhibit any flow discharge are either closed fractures or small fractures not connected to the fracture network. There are 146 fractures with the observed flow discharge. Figure 4 shows the traces of these fractures as well as the modelling domain, the horizontal monitoring borehole 12MI33 with 6 test intervals, and the vertical exploratory borehole MIZ-1.

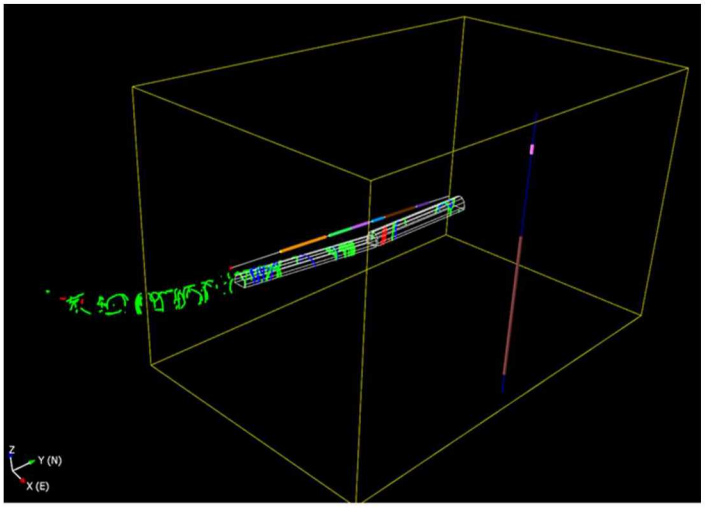

Figure 4. Modelling domain and traces of the fractures included in the analysis.

Fracture size was derived from trace length analysis. Trace length distributions of all sets are best described with the lognormal distribution. Fractures with observed inflows greater than 1 L/min have mean radius of 3.9 m (standard deviation 2.2 m). Fractures with smaller inflows have mean radius of 1.4 m (standard deviation 1.3 m).

The analysis assumed the following correlations between the fracture equivalent radius (R) and fracture permeability (k) and aperture (b):

$$k = \gamma_1 \cdot R^{\omega} \qquad (4.1.1.x.1\text{-}1)$$

$$b = \gamma_2 \cdot R \qquad (4.1.1.x.1\text{-}2)$$

where γ_1, γ_2, and ω are coefficients. The following parameters resulted in the best fit between the calculated and observed inflow into the tunnel: γ_1 =1.55x10^{-12}; γ_2 =1.16x10-5; and ω =2.3. The transmissivity estimates were corroborated by comparing the packer test results with the transmissivity of fractures generated in borehole 12MI33. Figure 5 shows the fractures generated in the borehole along with the Research tunnel fractures. The figure also shows the transmissivity of the test intervals obtained in the packer tests. The high transmissivity intervals 1, 2' and 6 coincide with the zones in which fractures generated in both the Research tunnel and borehole are present.

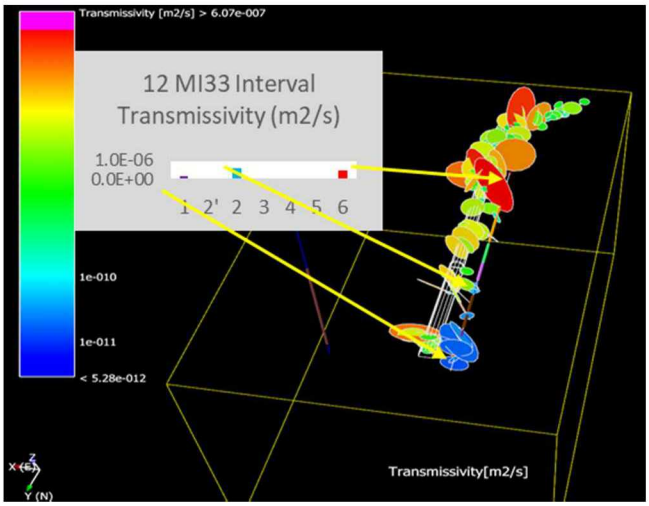

Figure 5. Transmissivity of fractures in the Research tunnel and borehole 12MI33.

The number of fracture sets and their orientation was obtained from the analysis of the fractures generated from the tunnel traces. Two fracture sets were unidentified. Their parameters are summarized in Table 1.

Table 1. Fracture Orientation Distributions.

Fracture Set	Trend (0)	Plunge (0)	Fisher Dispersion k	P32 (1/m)
Set 1	208	8	7	0.22
Set 2	303	1.3	3.6	0.086

To evaluate volumetric intensity P32 of each fracture set the following approach was used. The stochastic fractures were generated using Fisher distributions (Table 1), fracture radius distributions, fracture permeability (Eq. 4.1.1.x.1-1), and fracture aperture (Eq. 4.1.1.x.1-2). The P32 values were iteratively redefined until the linear intensity (P10) values in two arbitrary placed imaginary horizontal boreholes matched P10 of fractures observed in the Research tunnel and borehole 12MI33. The calculated P32 values are provided in Table 1.

Figure 6 shows one realization of the DFN generated with the properties defined in Table 1. The DFN model includes:

- Fractures observed in the Research tunnel and borehole 12MI33. These fractures have deterministic locations and stochastic (radius, permeability, and aperture) properties derived from the fracture analysis.
- Stochastic fractures (the location changes with each realization) generated based on the fracture size, orientation, intensity, and properties derived from the fracture analysis.

This DFN model was upscaled to a continuum model for simulating flow and transport. As shown in Section 4.1.2.x.2, a very good match between the observed and calculated inflow into the Research tunnel is obtained with this model.

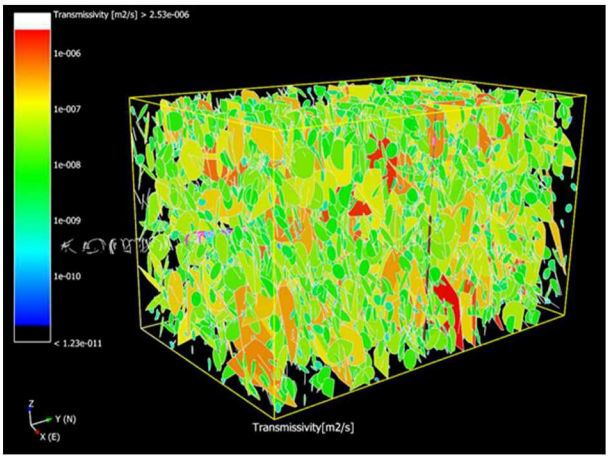

Figure 6. One realization of the discrete fracture network.

4.1.1.x.2 Fracture Data from Different Studies

Granite rocks have been studied worldwide for many different purposes. These purposes include mining (quarry development), contaminant transport, oil and gas exploration and others. The information from these studies can contribute to developing the fractured rock conceptual model. The studies include:

- Jizera Granite, Czech Republic (Zak, 2009)
- Soultz Geothermal Site, France (Dezayes, 2000 and Massart, 2010)
- Granite Site in Northern Spain (Klint, 2004)
- Kakkonda Granite, Kakkonda Geothermal Field, Northern Japan (Kato, 1999)
- Gebel El Zeit Basement Block, Egypt (Younes, 1998)
- Ten Granite Sites in North Eastern Portugal (Sousa, 2007)
- Vinalhaven Island Granite Site, Maine (Lorenz, 2007)

The following observations can be made from a review of these studies (Kalinina et al., 2012):

- In most cases, there are two predominant sets of sub-vertical fractures orthogonal to each other. Three or more sets are observed in some cases and are related to more complex tectonic (stress) history of the region. Sub-horizontal fractures are only observed at shallow depths and are due to erosion and stress release. These fractures are not expected to be present at greater depth intervals.
- Variations of fracture spacing at different sites are relatively small given the variety of site-specific conditions considered. Differences appear to be more set specific than site specific. Mean fracture spacing is from 0.3 m to 3.0 m. In most cases, the fracture spacing distribution follows either power law or exponential distribution. Maximum fracture spacing is less than 10 m. Greater than 10 m spacing is observed only in a few cases.
- Fracture spacing might be different for different sets. Fracture spacing varies with the distance from the faults (smaller spacing closer to the fault). Fracture spacing may vary with depth due to different granite rock types and ages (old versus young) and stress history.
- Observed fracture apertures range from 100 μm to 1,000 μm, except for fractures associated with faults, which have larger (up to 3,000 μm) apertures.
- Fracture length data are less extensive. However, there is some evidence that length may follow a power law distribution. This suggests that most of the fractures are small (less than 20 m). Only 5-10% of fractures are long (greater than 20 m with the maximum length of a few hundred meters). Fracture length and fracture spacing might have a positive correlation.

4.1.2. **Groundwater flow**

4.1.2.x USA

4.1.2.x.1 Representation of fractured rock using Discrete Fracture Network and Equivalent Continuum Models

Design of a nuclear waste disposal system in fractured crystalline rock requires a robust characterization of the fractured host rock. Various fracture modelling approaches have been employed to represent the fractured rock. The various approaches can be broadly divided into Discrete Fracture Network (DFN) and Equivalent Continuum Model (ECM) (Zhang and Sanderson, 2002). Both approaches are useful tools in modelling flow and transport.

The DFN approach is widely used in various applications, including nuclear waste disposal (e.g. Uchida et al., 1994; Dershowitz et al., 1998). In the DFN approach, networks of fractures are created where the geometry and properties of individual fractures are explicitly represented. Most DFN models assume that flow and transport only occur through the network with no participation of the rock matrix. In the model, each fracture is a two-dimensional planar object with specific shape and size and object-specific hydraulic properties such as transmissivity and aperture. If the location of a fracture is known, then the fracture can be deterministically included in the model. Otherwise, fractures are generated stochastically based on the probability distributions of fracture orientation and size derived from field observations.

The ECM approach is also used in different applications, including geothermal and nuclear waste disposal. In ECM, individual fracture properties are translated into the properties of an equivalent porous medium. The main goal of an ECM is to reproduce the behavior (e.g. flow and transport) of the corresponding fracture network. The ECM is commonly used when the number of fractures in the model domain is large and/or the interaction between the matrix and fractures is an important factor. Examples of the ECM approach are found in Hsieh et al., (1985), Neuman and Depner (1988), Carrera et al. (1990), Tsang et al. (1996), and Altman et al. (1996) Jackson et al. (2000), Hartley and Joice (2013), Kalinina et al. (2014) and Hadgu et al. (2016).

A comparative study of the DFN and ECM models can be found in Hadgu et al. (2017), and Wang et al. (2017). That study used the dfnWorks software from Los Alamos National Laboratory (Hyman et al., 2015) and the Fracture Continuum Model software from Sandia National Laboratories (Kalinina et al., 2014, and Hadgu et al. 2016). For the model comparison a benchmark problem was constructed to represent the far field of a hypothetical repository in fractured crystalline rocks using generic fracture properties. Stochastic methods were used to generate permeability and porosity fields for a selected number of realizations. Examples of the generated permeability and porosity fields are given in Figure 7and Figure 8. In the problem, groundwater flow is represented using a pressure gradient along two faces of modeling domain. A pulse tracer source is applied representing non-reactive transport. The numerical code PFLOTRAN (Hammond et al., 2014) was used to model flow and transport for the two models. Transport within the DFN was also simulated using a Lagrangian particle tracking code (Makedonska et al., 2015). The results show that both approaches can provide a reasonable representation of the fractured rock. Further details on the comparison can be found in Wang et al. (2017).

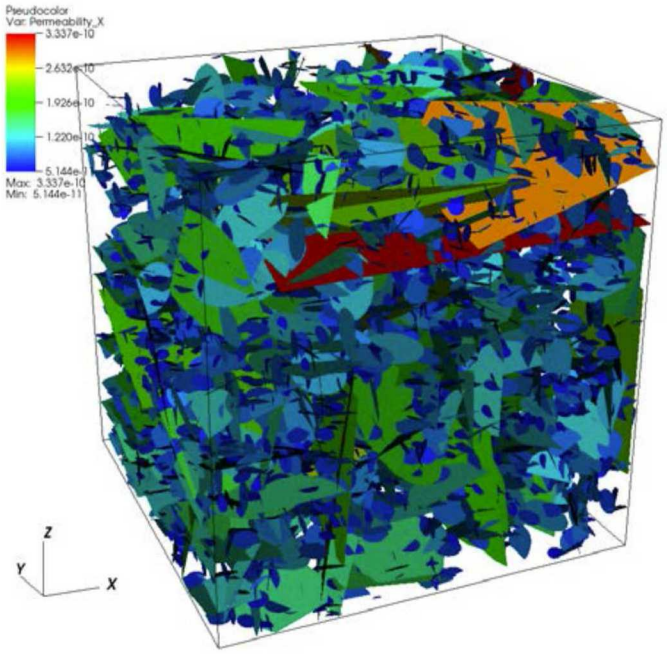

Figure 7. Representation of hydraulic conductivity of a DFN realization (Hadgu et al. 2017).

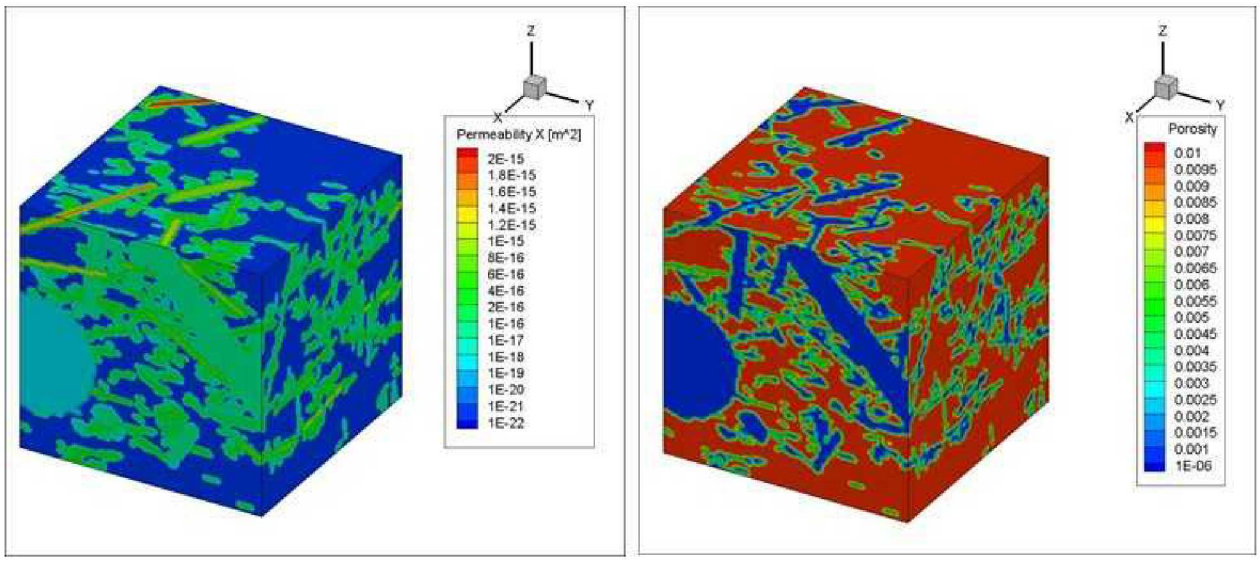

Figure 8. Representation of permeability (left) and porosity (right) of an ECM realization (Hadgu et al. 2017).

4.1.2.x.2 Mizunami Groundwater Recovery Experiment

The Mizunami Underground Research Laboratory (URL), located in Tono area (Central Japan), is a research facility administered by the Japan Atomic Energy Agency (JAEA). Description of the hydrogeology of the area can be found in Iwatsuki et al., 2005 and Iwatsuki et al., 2015. An experiment known as GREET (Groundwater REcovery Experiment in Tunnel) is being conducted at the URL to evaluate environmental conditions in fractured crystalline rock. The experimental gallery (Closure Test Drift) is located at 500 m depth with a volume of approx.

900 m^3. The experiments include flooding of the gallery and conducting repetitive drainage tests to ascertain reproducibility of hydraulic response. Figure 9 shows location and details of the research facility.

As part of the Development of Coupled Models and their Validation against Experiments (DECOVALEX19) project, three teams (JAEA, Sandia National Laboratories and Technical University of Liberec, Czech Republic) are studying the hydrological, chemical and mechanical conditions of the research area. What follows is a summary of the work of the Sandia National Laboratories team. The detailed work is documented in Wang et al. (2017).

A comprehensive set of fracture, hydrologic and chemical data was obtained based on experiments in the research tunnel. A discrete fracture network was developed based on fracture data collected from the excavated areas and boreholes. Development of the DFN model is described in Section 4.1.1.x. The fracture data analysis produced upscaled permeability and porosity data for flow and transport modeling. The modeling work as part of DECOVALEX19 is done in steps. In this report we discuss the modeling work that was done to predict inflow of water into part of the tunnel as the tunnel is excavated. Figure 10 shows the experimental data representing the progress of the excavation process.

Preliminary modeling analysis was conducted for a homogenous model with reference hydraulic conductivity, and a fracture model. The simulations used a 100 m x 150 m x 100 m domain. A uniform grid with grid block size of 1 m x 1 m x 1 m was used for a total mesh size of 1,500,000 grid blocks. Boundary and initial conditions specified by the project, based on data from wells, were applied to flow and transport (see Figure 11). The data include head and chloride concentration at different parts of the modeling domain. Parameter data also obtained from wells were used. A simulation method was developed to simulate excavation progress by continuously removing material from the excavated area. The Dakota statistical analysis and optimization code (Adam, et al., 2017) and the PFLOTRAN numerical flow and transport code (Hammond et al., 2014) were used.

The modeling analysis also included use of a fracture model with upscaled permeability and porosity fields. This allowed realistic representation of the fractured rock in the simulation domain. The same simulation approach as the homogenous model was followed. The simulation results provided detailed flow and transport distributions in a fractured system. Both the homogenous and fracture models were used to predict inflow of water as the tunnel was excavated and pressure and chloride concentrations at specified observation points. Figure 12 shows predictions of inflow using the two models as wells as experimental data points. The results show that the inflow predictions of the fracture model were closer to the experimental data.

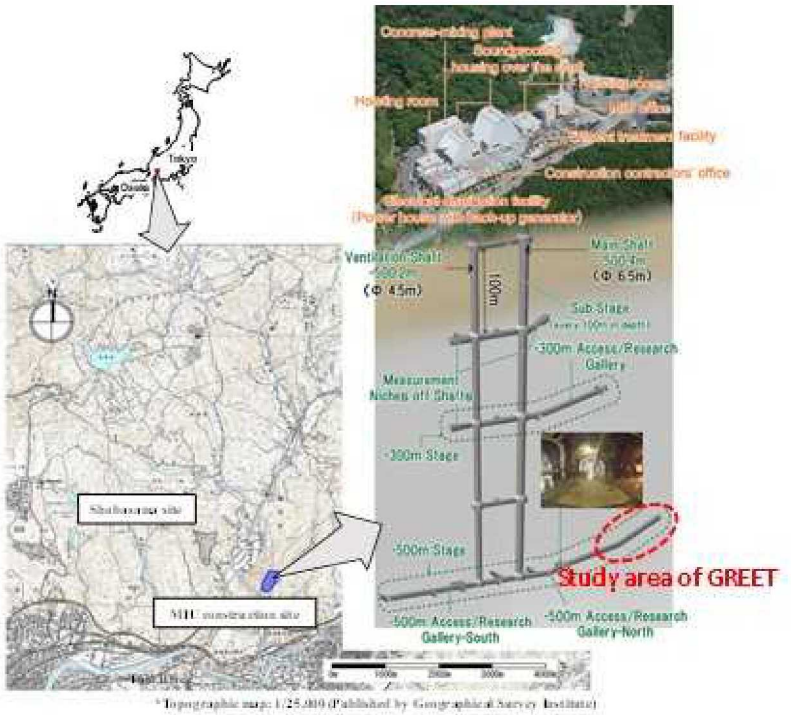

Figure 9. Location and layout of the Mizunami Underground Research Laboratory (Wang et al. 2017).

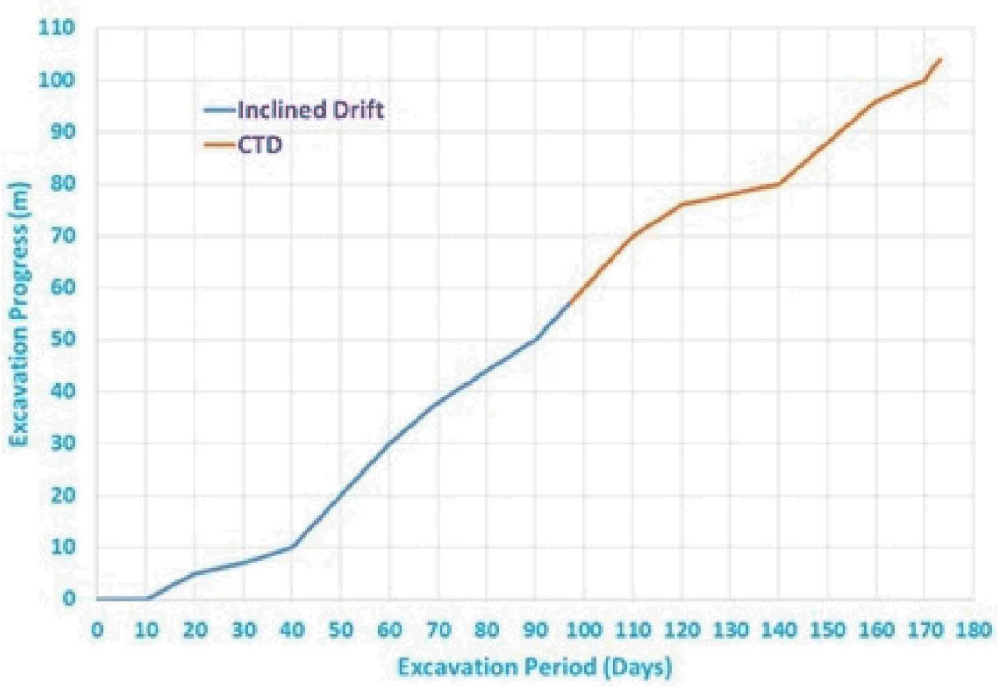

Figure 10. Data of tunnel excavation progress (Wang et al. 2017).

.

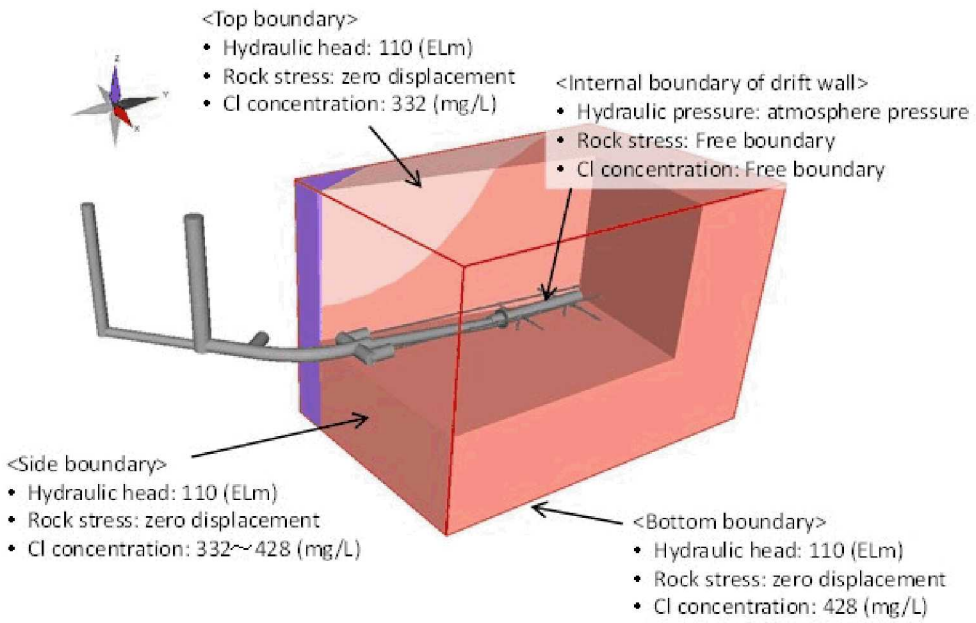

Figure 11. Boundary condition for numerical simulation (Wang et al. 2017).

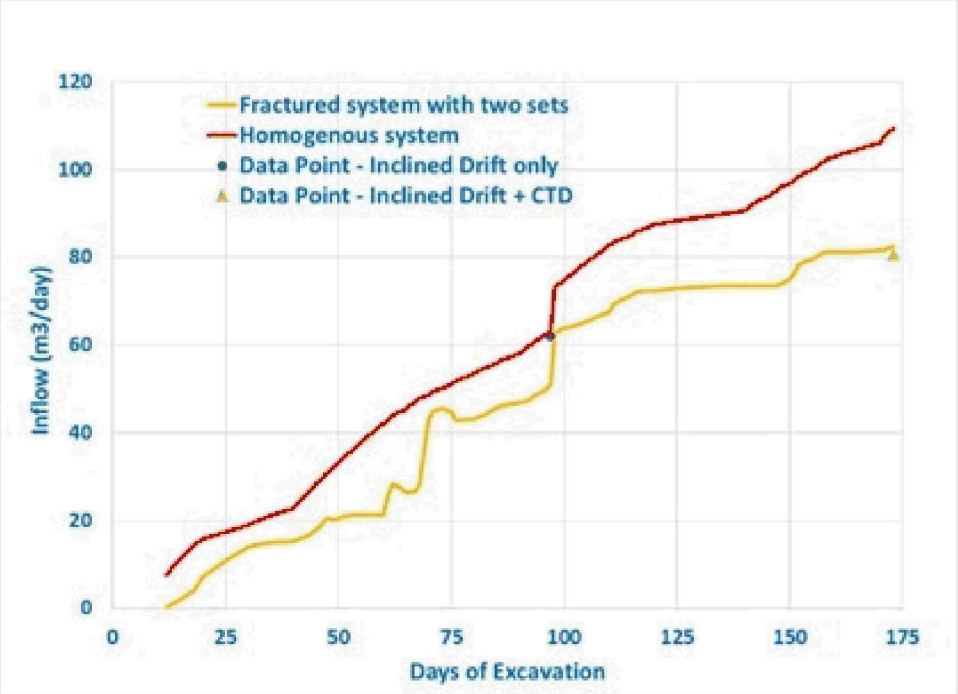

Figure 12. Predicted inflow into Inclined Drift and CTD: Comparison of results of Homogenous and Fracture Models with experimental data.

4.1.3. Hydrogeochemistry

4.1.3.x USA

Disposal R&D activities under the US DOE SFWST campaign have produced state-of-the-art modeling capabilities for coupled Thermal-Hydrological-Mechanical-Chemical (THMC), thermodynamic modelling, and database development to evaluate generic disposal concepts (Jove Colon et al. 2013, 2014). Thermodynamic data are key to the evaluation of geochemical processes and solid-fluid interactions in many environments, for example, in speciation-solubility calculations at low and high temperatures, reaction-path modelling, or porous media reactive transport simulations. Critically-assessed thermodynamic data are required to evaluate solution-mineral equilibria. The relevance to nuclear waste disposal R&D is the application of such calculations to the evaluation of interactions involving barrier materials such as metal alloys, bentonite clay, and cementitious barriers. Waste form degradation, engineered barrier system performance, and near-field and far-field transport typically incorporate some level of thermodynamic modelling to assess material performance in long-term nuclear waste isolation.

Thermodynamic database development has a long history in geochemistry (e.g., Garrels and Christ, 1965; Helgeson et al., 1969; Helgeson et al., 1978, Johnson et al., 1992; Robie and Hemingway, 1995), paralleled by related and applicable work in the larger scientific community (e.g., Wagman et al., 1982, 1989; Cox et al., 1989; Barin and Platzki, 1995; Binneweis and Milke, 1999). IUPAC, whose efforts in this area were generally limited to data pertaining to key species only (a small subset), has not done much in this area since the publication of the Cox et al. (1989) report. The standards organizations have been largely inactive regarding thermodynamic data of interest to geochemical and repository studies for over twenty years. For radionuclide and other elements, much of this void has been filled by the European Nuclear Energy Agency (NEA), which has sponsored a series of review volumes (e.g., Grenthe et al., 1992 [1: uranium]; Silva et al., 1995 [2: americium]; Rard et al., 1999 [3: technetium]; Lemire et al., 2001 [4: neptunium and plutonium]; Guillaumont et al., 2003 [5: update on uranium, neptunium, plutonium americium, and technetium]; Gamsjäger et al., 2005 [6: nickel]; and Olin et al., 2005 [7: selenium]).

Many thermodynamic database developments commonly used in the geochemistry community builds on the work of Prof. Helgeson and his students (see BSC, 2007a), encompassing a significant range of pressures and temperatures. The SUPCRT92 database supports "HKF equation of state" models (first developed by Walther and Helgeson, 1977; Helgeson and Kirkham, 1976; and Helgeson et al., 1981) to calculate Gibbs energies and associated functions for aqueous solute species at elevated temperatures and pressures. The revised HKF treatment has been revised and expanded in terms of chemical species (Shock and Helgeson, 1988; Shock et al., 1989; Shock et al. 1997). Applications of the HKF model is still widespread in the geochemical community (see for example Dolejš and Baker, 2004; Dolejš and Wagner, 2008; Sverjensky et al., 2014; and Miron et al., 2016). Efforts toward the improvement of thermodynamic databases are continuing, with some targeting the inclusion of additional chemical species, extending the range of temperatures and pressures, approaches to represent non-ideality, and testing and increasing accuracy along with consistency. Some recent works along this path of thermodynamic database development include Heinrich et al., 1996; Dolejš and Wagner (2008), Holland and Powell (2011), Dolejš (2013), Sverjensky et al. (2014), Tutolo et al. (2014), and Miron et al. (2016).

Emphasis on the progress in the development of thermodynamic databases (TDBs) relevant to geochemical processes has been on the needs for data updates/corrections based on new estimates of thermodynamic properties of various complex clays and related sheet silicates. These groups of minerals are key to nuclear waste disposal since these are the main components of the engineered barrier system (EBS) such as bentonite clay, and the natural host-rock barrier in the case of disposal in clay rock (e.g., argillite). Assessing the needed revisions leads to the necessary re-evaluation of the widely-used Helgeson et al. (1978) dataset along with data retrieval methodologies with a similar but the more modern one of Holland and Powell (2011). The resolution of key data issues and inconsistencies are therefore necessary for applications to nuclear waste disposal, particularly on the accurate prediction of mineral solubilities and phase relations at elevated temperatures. In this respect, inconsistencies with primary key reference data (standard Gibbs energies, standard enthalpies, and standard entropies for key chemical species) are still an issue in some data compilations. To assess these inconsistencies, Wolery and Jové Colón (2017) proposed a concept involving "links" to the elemental reference forms. This involves the evaluation of all reactions along with calculations leading to documented values for a standard thermodynamic property of formation (e.g., Gibbs energies, enthalpies).

Currently, the use of large waste packages (e.g., dual purpose canisters (DPCs)) is being considered in the US nuclear waste disposal. These large canisters can hold up to 32 PWR assemblies, therefore generating high thermal loads with temperatures of up to nearly 300°C. Such high temperatures on bentonite backfill material can exert large effects on barrier material interactions (e.g., steel-clay interface), mineral phase transformation, and thus solution-mineral equilibria (see Cheshire et al. 2014). As a result, there is an increased focus on chemical interactions at high temperatures involving silicates and metallic phases comprising engineered barrier materials. Consequently, the need to conduct such analysis also falls into the development of thermodynamic databases to support this type of calculations.

4.1.4.Solute transport

4.1.4.x USA

4.1.4.x.1 Colloid-facilitated transport at Grimsel test site, Switzerland

Understanding colloid-facilitated radionuclide transport in granitic materials is an important component of the evaluation of the natural and engineered barrier systems. One of the radionuclides of interest is cesium which is a health hazard even in trace concentrations. Transport experiments using two mini-columns were conducted to study the colloid-facilitated transport of ^{137}Cs through crushed Grimsel granodiorite at the Grimsel test site, Switzerland. Wang et al. (2017) provides a detailed analysis of the study conducted at Los Alamos National Laboratory. A summary of the work is discussed below.

For the colloid-facilitated transport study, water from the Chancellor nuclear test cavity at the Nevada Nuclear Security Site was selected because ^{137}Cs is strongly associated with the colloidal fraction and ^{3}HHO is present in high concentrations and therefore acts as a conservative tracer. Column eluent was measured for ^{3}HHO, ^{137}Cs, and turbidity (as a proxy for colloid concentration). After one pore volume eluted through the first column, both the ^{3}HHO and turbidity reached Chancellor water values, suggesting that no colloids were filtered by the granodiorite.

Experimental breakthrough curves are shown in Figure 13 and Figure 14. ^{137}Cs breakthrough occurred concurrently with the ^{3}HHO and turbidity breakthroughs but in concentrations less than the injection solution. The initial breakthrough consisted almost entirely of colloidal ^{137}Cs. Solute concentrations of ^{137}Cs were negligible initially and rose steadily along with the colloid-associated ^{137}Cs until about 50 pore volumes, after which both solute and colloid-associated ^{137}Cs eluted through the column at the same concentration and partitioning as the injection solution, suggesting that the granodiorite's adsorption capacity had been exhausted. Eluent samples from the first ~26 pore volumes that were not used for analysis were combined and injected into a second column. Analyses indicated that the granodiorite in the first column had adsorbed most of the ^{137}Cs in the solute phase and over half of the ^{137}Cs that was associated colloids during the first 26 pore volumes. Thus, the injection solution into the second column consisted mainly of ^{137}Cs strongly bound to colloid surfaces that outcompeted the sites of the granodiorite.

The results from the second column reflect the much stronger association between the ^{137}Cs and the strong sites of the colloids. In contrast to the results from the first column, where only about 45% of the ^{137}Cs initially associated with colloids remained associated with colloids, about 90% of the colloid-associated ^{137}Cs remained associated with colloids in the second column. The results from both column experiments were simultaneously matched by a two-adsorption-site model in which the first site is weaker than the second but has greater abundance. These experiments demonstrate how the sequential column technique can provide well-constrained model parameterizations of the adsorption and desorption behavior of a radionuclide on colloids in the presence of competing immobile surfaces. The method is especially well suited to interrogate the slower desorption rate constants of radionuclides from colloids that will dictate the magnitude of colloid-facilitated radionuclide transport over the long time and distance scales relevant to nuclear waste repository systems.

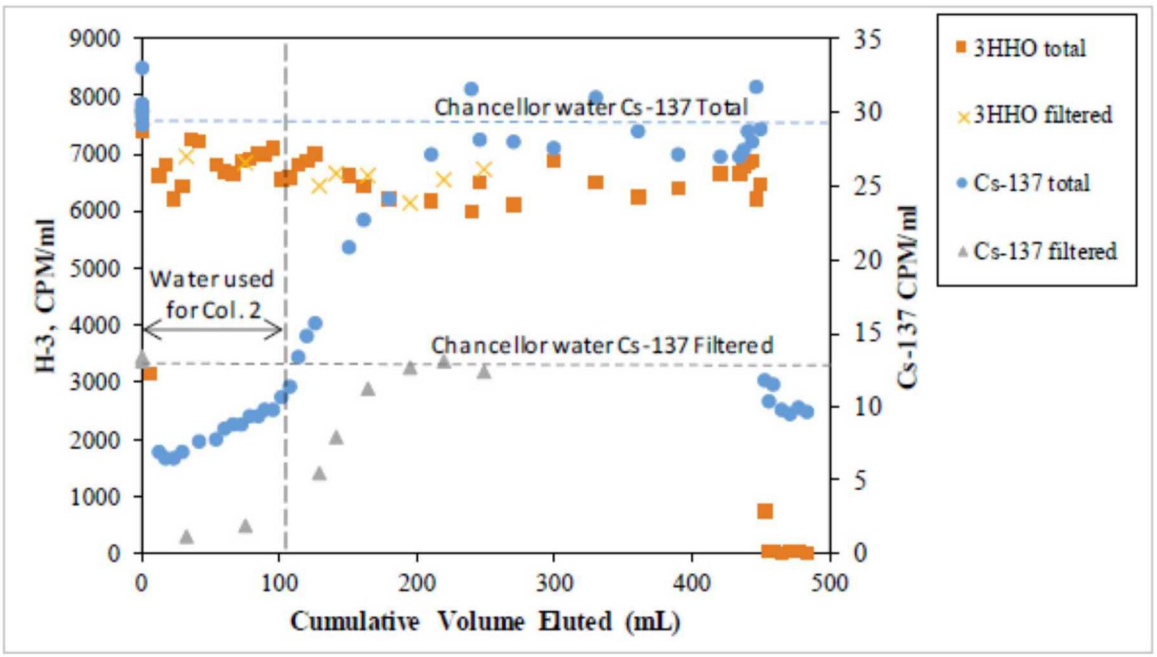

Figure 13. Measured breakthrough curves of ^{3}HHO and ^{137}Cs in Column 1 (Wang et al. 2017).

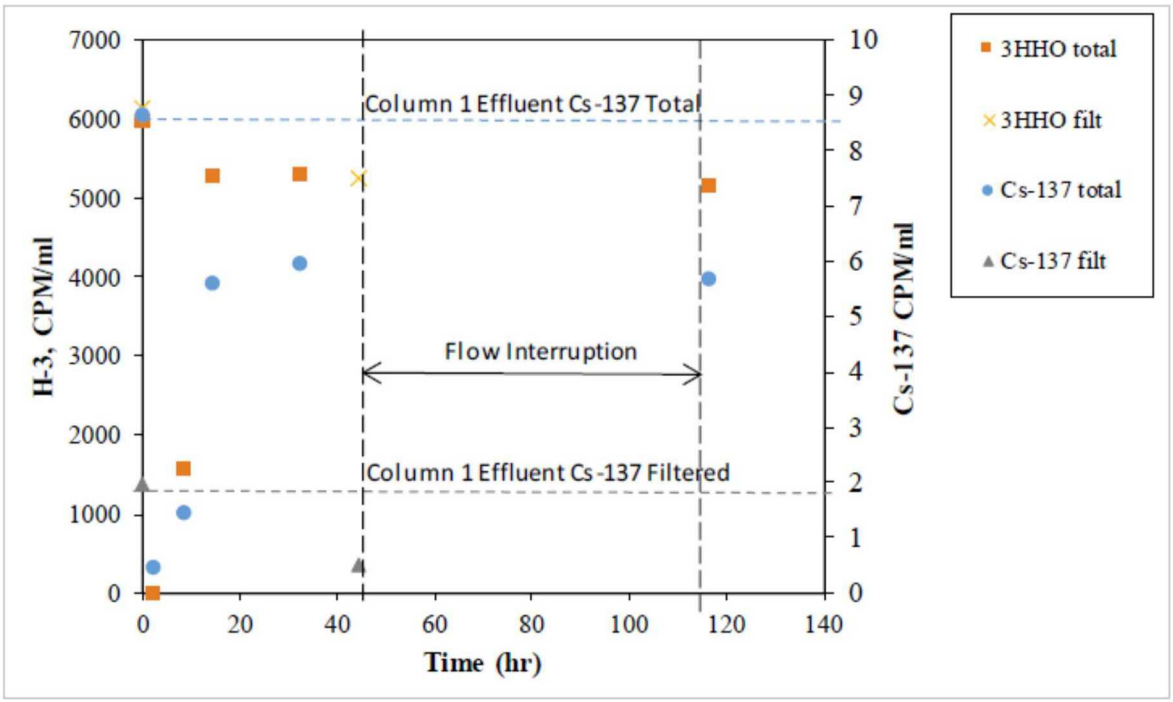

Figure 14. Measured breakthrough curves of ^{3}HHO and ^{137}Cs in Column 2 (Wang et al. 2017).

4.1.4.x.2 Solute transport modeling for Swedish Long-Term Diffusion Experiments

A study of solute dispersion and mixing in fracture networks was conducted at Los Alamos National Laboratory. Details of the study are given in Wang et al. (2017). A summary of the work is shown below.

A DFN model was applied to interpret tracer diffusion data obtained from the Long-Term Sorption Diffusion Experiments conducted in Sweden. Experiments were focused on tracer transport in the stagnant pore water of the rock matrix. Analyzing the shape of the tracer penetration profiles observed in the experiment and comparing it to the predicted general shape of a 1D diffusion model, vastly different behavior was observed for the natural fracture surfaces and for the unaltered rock matrix. The micro fractures were observed in different slices of the sample core. Several slices of the individual cores had micro fractures that were fresh and consequently they were likely newly formed, i.e., induced by drilling or stress release. The current study focuses on understanding how micro fractures, which provide faster transport paths, affect the penetration profile. The DFN model was used to investigate, how the thickness of the fractured layer affects the penetration profile of tracer driven by pure diffusion. The results emphasize the importance of including heterogeneity in the simulation process. Micro fractured surface contributes to initial fast decrease of concentration followed by a slower penetration as tracer gets into homogeneous medium.

A DFN model was used to investigate, how the thickness of the fractured layer affects the penetration profile of tracer driven by pure diffusion. The dfnWorks software (Hyman et al., 2015) was used for micro fracture modeling. To include diffusion into the rock matrix, a new method of mapping of DFN onto a high-resolution continuum mesh was developed. This new capability was used to study the effect of micro fractures on diffusive transport.

The DFN was generated according to Äspö, Sweden site characteristics for the fracture data (Table 2), with slight modifications for micro-structure modeling:

- Domain size is 5 cm × 5 cm × 5 cm; total volume 125 cm^3.
- All fractures size follows a power law distribution, where smallest fracture length is 1 mm and longest fracture length is 1 cm.
- All fractures in the DFN are connected and provide a connected path through fractures for transport.

In the DFN model, fractures represent porous paths between grains. To include the diffusion process between fracture surface and grains, the generated DFN was mapped onto a continuum mesh as shown in Figure 15 with mapped fracture network. Each voxel has a dimension of 0.2 mm^3, which is 5 times smaller than the shortest fracture length. The main parameter that is being translated from DFN to continuum is porosity. The obtained continuum mesh consists of 250 x 250 x 250 hexagonal units. Figure 16 shows an example of a DFN mapped into a continuum. The thickness of the fractured coating on the sample can be different and the damaged surface thickness can vary. In the model, 7 different variations in 50 mm intervals between the external surface and the sample center: from 10 mm to 40 mm with a step of 5 mm, moving from surface to the center. The center of the sample remains the unaltered rock with porosity 0.003.

The massively parallel multi-physics code, PFLOTRAN (Hammond, 2014), was used to simulate pure diffusion of tracer from top to bottom, from fractured surface to sample center. Dirichlet boundary conditions were applied to the top surface; and zero gradient boundary condition was assumed at the bottom so that the tracer cannot go through the bottom face, which is the sample center.

Figure 17 shows the tracer penetration at 200 days of diffusion simulations for the case of 40 mm of fractured surface. The heterogeneity of tracer movement is clearly observed at fractured layers due the presence of micro fractures and the difference in porosities, even though only diffusion is considered in these simulations.

Figure 18 shows penetration profile of tracer driven by diffusion for 200 days. The combination of both fractured layer and unaltered rock matrix results in different behavior than was observed in the previous diffusion simulations. As the fractured layer increases, the concentration is lower at the same depth due to a porosity increase at the damage surface. The behavior of the system shows better qualitative agreement to the experiments compared to the 1D diffusion simulation where heterogeneity due to micro fractures was not considered.

The results emphasize the importance of including heterogeneity in the simulation process. Microfractures contribute to initial fast decrease of concentration followed by a slower penetration of tracer into the homogeneous medium.

Table 2. DFN input parameters

Set	Trend	Plunge	Kappa	R_{Min} (m)	R_{Max} (m)	Alpha	P_{32}
1	280	20	10	0.0005	0.005	2.6	750
2	20	10	15	0.0005	0.005	2.6	1000
3	120	50	10	0.0005	0.005	2.6	500

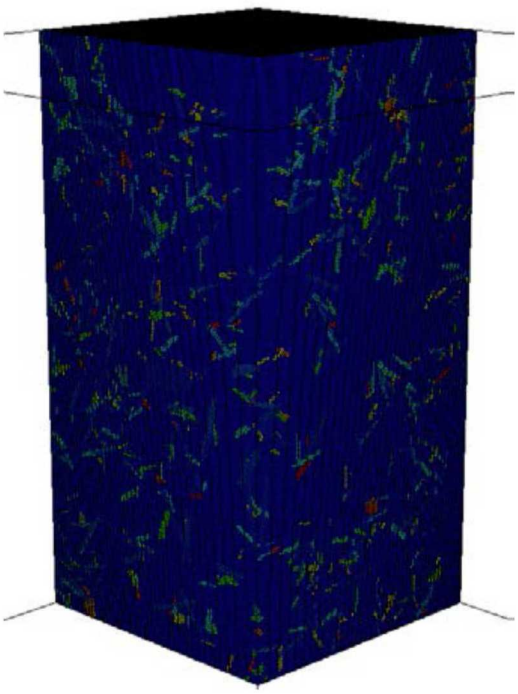

Figure 15. Slice of the obtained continuum mesh with mapped fracture network.

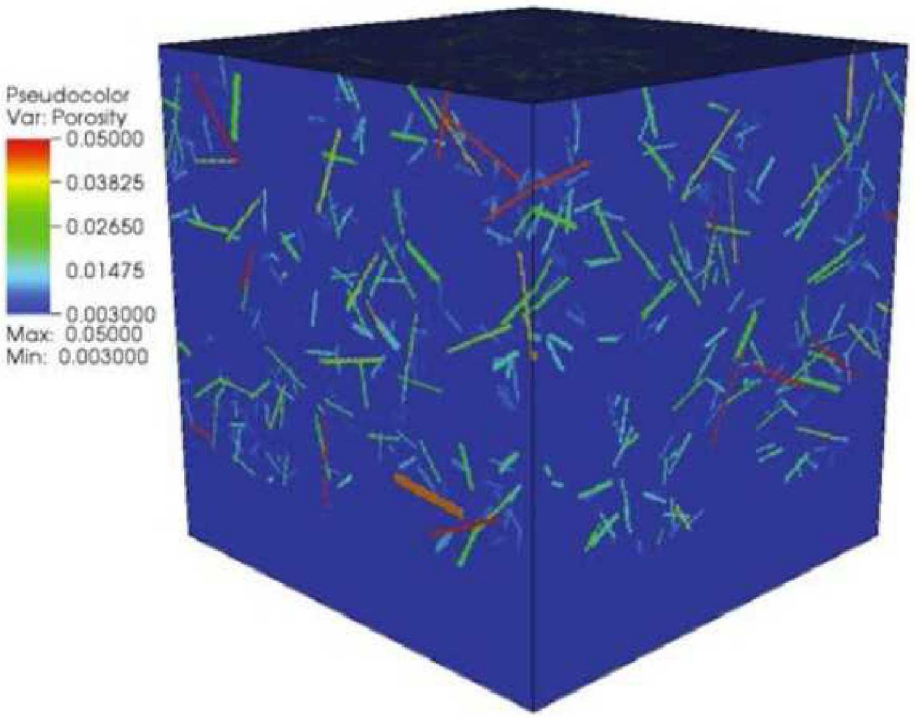

Figure 16. Example of a DFN mapped onto a continuum mesh. Colors represent cell's porosity. Fracture porosity vary from 0.05 to 0.005, and rock matrix porosity is 0.003.

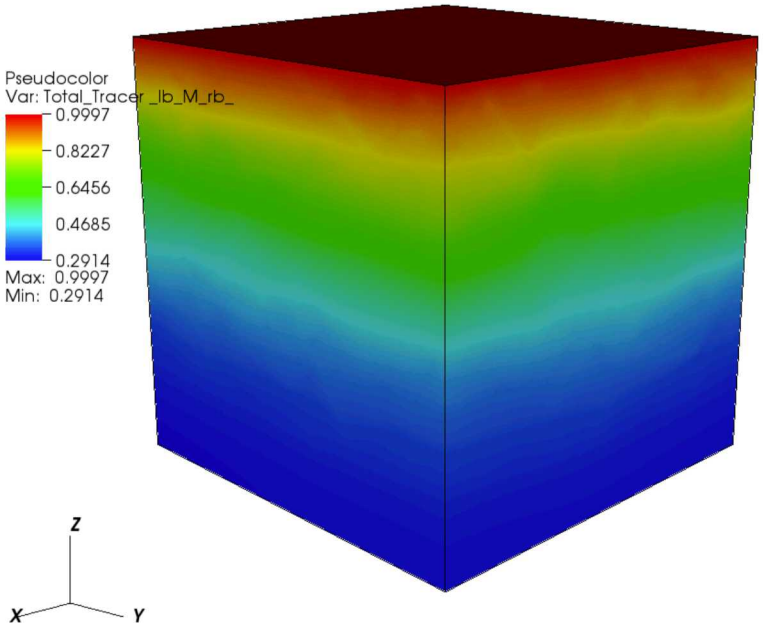

Figure 17. The tracer penetration at 200 days of diffusion simulation. Fractured surface thickness is 40 mm.

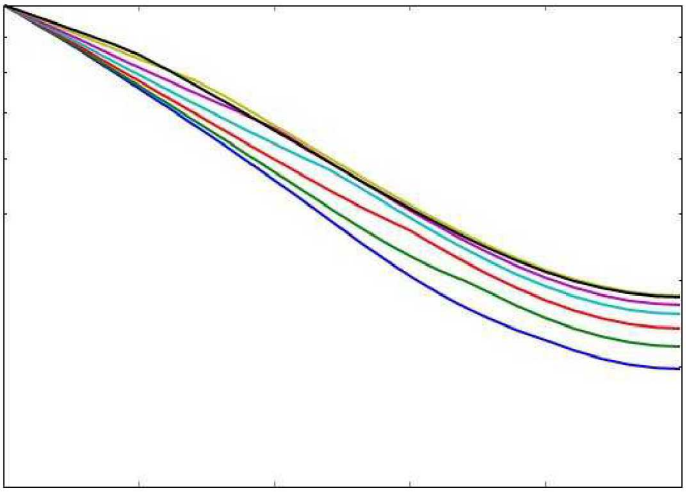

Figure 18. Penetration profile of tracer concentration in 200 days of diffusion simulations.

4.1.5. Mechanical and thermal properties

4.1.5.x USA

No contribution. US contributors focused on other sections of this report.

4.1.6. Long-term site stability

4.1.6.x USA

No contribution. US contributors focused on other sections of this report.

4.2. Laboratory research

4.2.1. Sorption properties in fractures engineered barriers, sealing and backfilling measures in crystalline rock mass, of fracture filling material and crystalline rocks

4.2.1.x USA

4.2.1.x.1 FEBEX dismantling project

The FEBEX (Full-scale Engineered Barrier Experiment in Crystalline Host Rock) project is a large-scale heater test experiment originated by the Spanish radioactive waste management agency (Empresa Nacional de Residuos Radiactivos S.A. – ENRESA) at the Grimsel Test Site (GTS) URL in Switzerland. The project was subsequently managed by CIEMAT. FEBEX-DP is a concerted effort of various international partners working on the evaluation of sensor data and characterization of samples obtained during the course of this field test and subsequent dismantling. The main purpose of these field-scale experiments is to evaluate feasibility for the creation of an engineered barrier system (EBS) with a horizontal configuration according to the Spanish concept of deep geological disposal of high-level radioactive waste in crystalline rock. Another key aspect of this project is to improve the knowledge of coupled processes such as thermal-hydro-mechanical (THM) and thermal-hydro-chemical (THC) operating in the near-field environment. The focus of these is on model development and validation of predictions through model implementation in computational tools to simulate coupled THM and THC processes. Figure 19 depicts the layout for the FEBEX "in situ" test with the heater zones. The FEBEX bentonite (blocks) is composed of 93% smectite with 2% quartz, 3% plagioclase, and 2% cristobalite plus minor accessory phases such as calcite and K-feldspar (Huertas et al. 2000; Missana and García-Gutiérrez 2007).

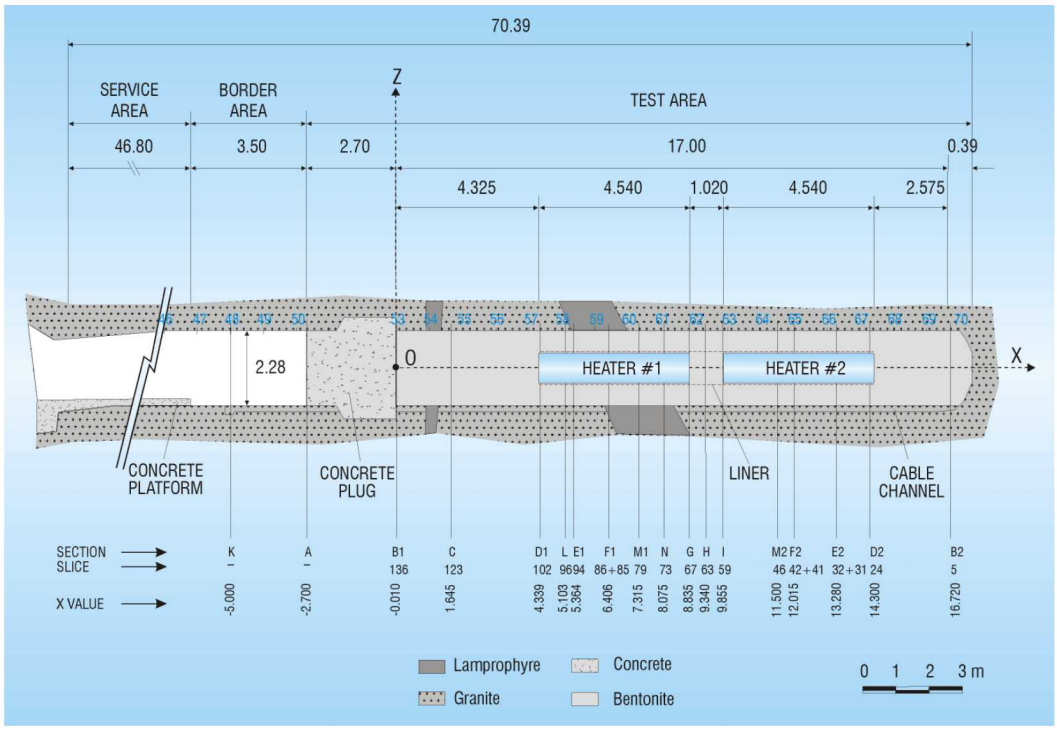

Figure 19. Schematic layout of the FEBEX "in-situ" test for the FEBEX I configuration at the GTS URL (ENRESA, 2000).

The current phase of FEBEX-DP focuses on the dismantling of heater #2 (see Figure 20) conducted during 2015 with the goal of disassembling all the remaining sections of the FEBEX "in situ test" after 18+ year of heating and sensor/probe data (García-Siñeriz et al. 2016; Martinez et al. 2016). This dismantling activity involves sampling of barrier bentonite, steel liner, sensors, embedded metallic components (e.g., metal coupons), and near-field sections with tracer components. Figure 21 shows the sampling zones for FEBEX-DP. Sampling of barrier materials included bentonite blocks with distance from heater, supporting steel liner, and concrete plug. Given the time length for this field experiment, it provides a unique opportunity to conduct research and evaluate the fate of barrier components under repository conditions. It should be noted that a previous partial dismantling of FEBEX heater #1 was conducted after 5 years while heater #2 continued operating without disruption. Also, Post-mortem analyses of concrete plug samples were obtained to evaluate physical, chemical, mineralogical, and textural changes after the initial dismantling operation (13 years). Details regarding the FEBEX-DP project can be found at the GTS website http://www.grimsel.com/gts-phase-v/febex/febex-i-introduction-.

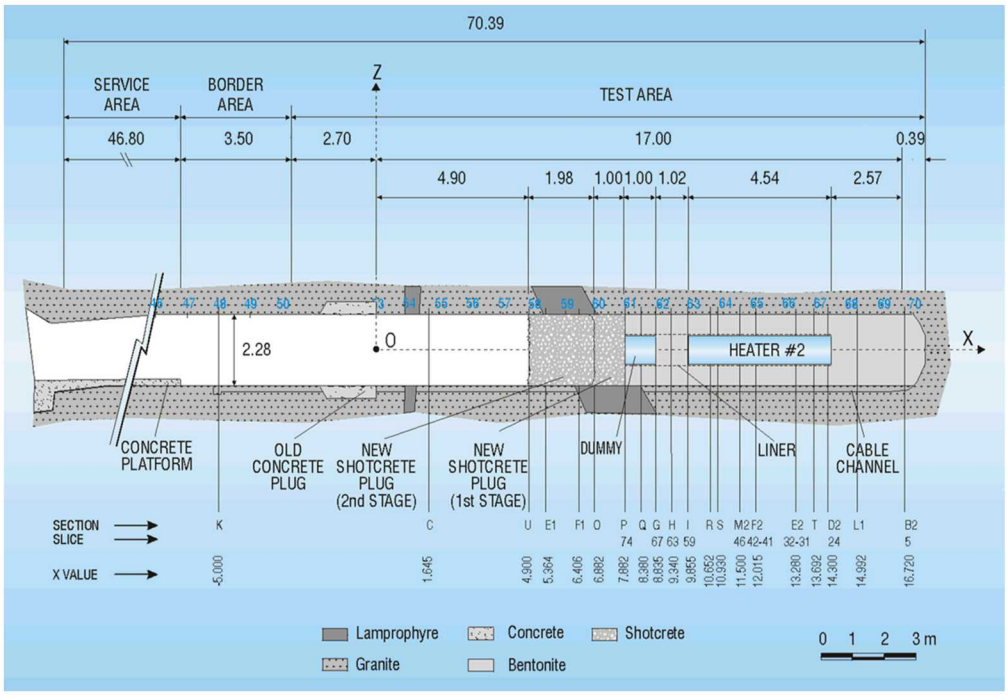

Figure 20. Schematic layout of the FEBEX "in-situ" field test after the first partial dismantling showing the configuration of heater #2 at the GTS URL (García-Siñeriz et al. 2016).

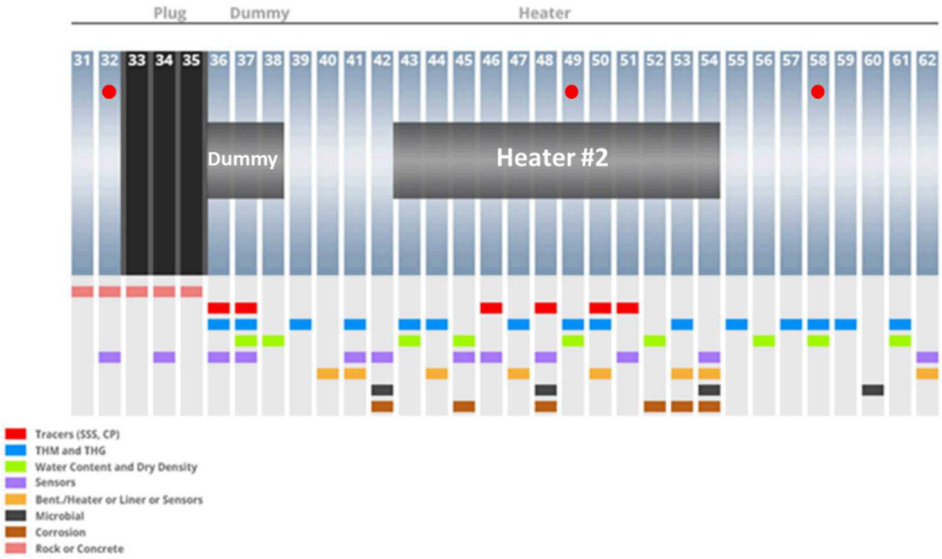

Figure 21. Schematic configuration of sampling zones (indicated by vertical light blue bars) for the FEBEX-DP project. Filled red circles indicate zones for samples obtained by Sandia National Laboratories (SNL). Source: FEBEX-DP website (members area): http://www.grimsel.com/gts-phase-vi/febex-dp/febex-dp-introduction.

4.2.1.x.2 The Mont Terri Underground Research Laboratory (URL) FE experiment

The Mont Terri Project is an international research project to study the hydrogeological, geochemical, and geotechnical properties of the Opalinus Clay formation at the Mont Terri URL in Switzerland. Many field experiments have been conducted at the Mont Terri URL but the following information, taken from SFWST milestone deliverable SFWD-SFWST-2017-000040 of the US DOE SFWST campaign (Zheng et al. 2017), is focused on the FE (full-scale) heater experiment to be undertaken by NAGRA. The FE heater test experiment is relevant to US DOE disposal concepts

given its overall target temperatures of above 100°C and its relatively large scale. It is also relevant to crystalline repository concepts because it will examine the THMC effects of high temperature on buffer evolution.

The FE experiment will be conducted in a 50-m long, 2.8-m diameter side tunnel at Mont Terri. Three heat-producing canisters emplaced in the tunnel will cause the temperature to exceed 100°C, with a target temperature 125 to 135°C in the buffer nearest the canisters.

US DOE is one of the experimental partners for the FE heater experiment. The THM modelling program includes three types of computations: 1) scoping calculations and benchmarking, 2) predictive modelling, and 3) interpretative modelling. For the computations, each modelling team will develop its own conceptual models and material properties.

4.3. Grouting technology

4.3.x USA

No contribution. US contributors focused on other sections of this report.

4.4. EDZ

4.4.x USA

4.4.x.1 Generating Fractures in the Research Tunnel at the Mizunami Underground Research Laboratory

Developing a fracture model around the EDZ is a challenging task. While fracture traces can be mapped on the walls of the tunnel, fracture size and shape remain unknown. Fracture apertures observed on the wall may not be representative of the actual fracture apertures inside the rock mass. The example considered below demonstrates the development of a fracture model around the research tunnel at the MIU.

Two thousand and twenty three fractures were mapped on the wall of the research tunnel (Figure 22). The fracture apertures were not recorded. The fractures were characterized in the original data set based on the flow range as "flow" (F) fractures (>1 L/min), "drop" (D) fractures (>0.1 L/min), "wet" (W) (<0.1 L/min) fractures, and NA fractures (insignificant flow). F, D, and W fractures were assumed to be connected to the fracture network (Table 3).

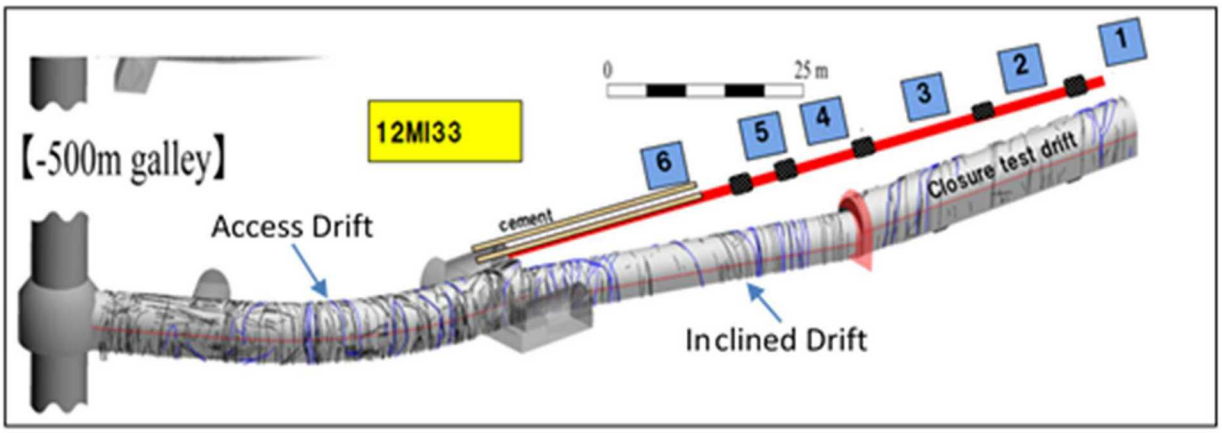

Figure 22. Observed fracture traces in the research tunnel.

Table 3. Research tunnel fractures included in the fracture analysis.

Research Tunnel Area	F-Fractures (flow>1.0 L/min)	D-Fractures (flow>0.1 L/min)	W-Fractures (flow<0.1 L/min)	All Fractures with Flow
CTD	4	15	3	22

Inclined Drift	14	42	N/A	56
Access Drift	N/A	65	3	68
Total	18	122	6	146

Fracture size was derived from trace length analysis using FRACMAN (Golder Associates, Inc., 2017). It was assumed that the fractures with different flow discharges have different sizes. Consequently, the analysis was conducted separately for F, D, and W fractures. FRACMAN uses an algorithm described in Zhang (2002) and La Pointe (2002) to estimate fracture size (equivalent radius) from trace length and offers different probability distributions for fitting data. The power-law and lognormal distributions were considered in this analysis. The lognormal distributions resulted in the best fits (Figure 23).

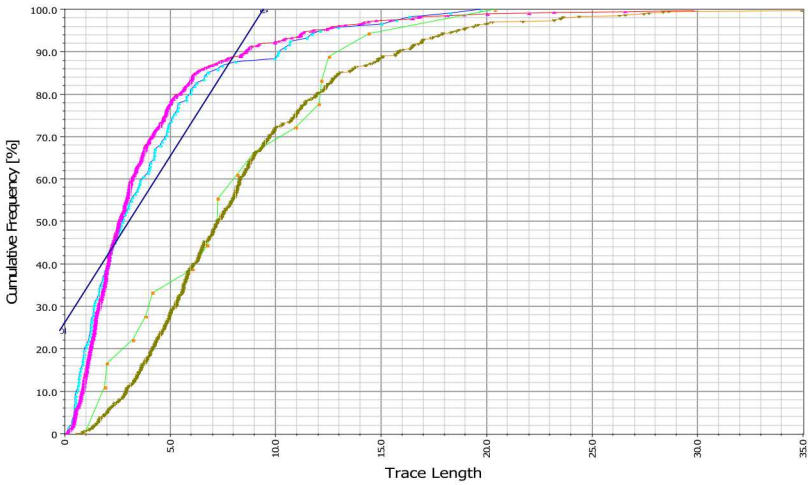

Figure 23. Lognormal distribution fit to the fracture trace data.

One hundred and forty-six fractures were generated in the research tunnel using the lognormal distributions for the equivalent fracture radius. Note that while the fracture location is fixed, fracture size will vary from realization to realization. Figure 24 shows the generated fractures for one realization.

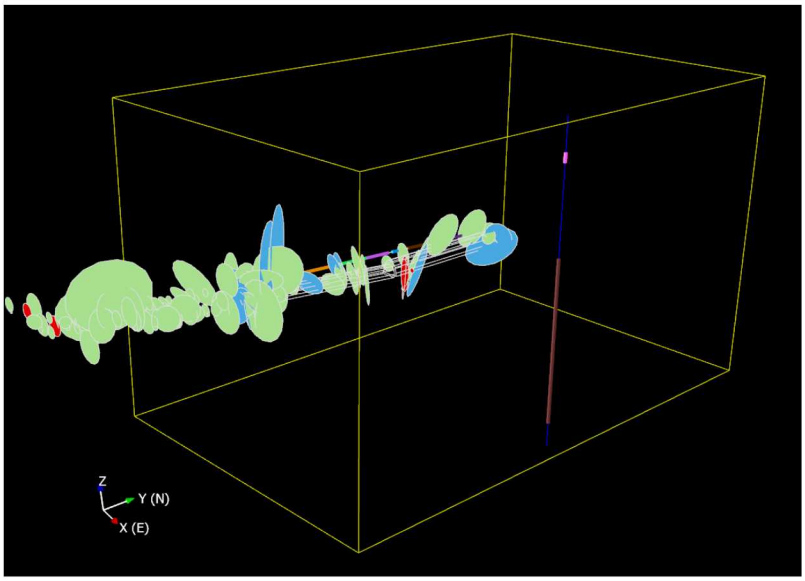

Figure 24. Fractures generated for one realization.

The initial evaluation of fracture transmissivity was based on the observed range of flow through the different types of fractures. The analytical solution for the unit inflow into a circular tunnel (Butscher, 2012) was modified to describe the inflow into a fracture. This equation was used to calculate fracture transmissivity. The transmissivity of F fractures was determined to be > $2.6*10^{-8}$ m^2/s. Ranges for the smaller D and W fractures were determined to be > $2.6*10^{-9}$ m^2/s and < $2.6*10^{-9}$ m^2/s, respectively.

The observed inflows into the Closure Test Drift and Inclined Drift were used to adjust these limits until a good match between the observed and calculated inflows was obtained.

The following ranges were derived for the fracture parameters:

- Fracture transmissivity: 2.6×10^{-9} – 6.0×10^{-8} m^2/s.
- Fracture permeability: 1.8×10^{-11} – 1.5×10^{-10} m^2
- Fracture aperture: 15 – 42 μm

It was shown that incorporating the known fractures into the DFN reduces uncertainty in evaluating inflow into the tunnel.

5. Safety functions of the geosphere & performance requirements of EBS

5.1. Thermal

5.1.x USA

US DOE is investigating the thermal limits of buffer materials. A 100°C thermal limit appears to be too restrictive (Jové Colón et al. 2012; Liu et al. 2013). Reviews of the performance of bentonite backfill at temperatures above 100°C and as high as 300°C (Wersin et al. 2007; Pusch et al. 2010), modelling (Liu et al. 2013; Zheng et al. 2014), and experimental studies (Pusch et al. 2003; Caporuscio et al. 2012; Cheshire et al. 2013; Wang et al. 2013; Cheshire et al. 2014) describing the mechanical and chemical changes showed little or moderate deterioration of bentonite. While added analyses of the thermal-hydrological-mechanical-chemical (THMC) alteration of EBS bentonite at high temperatures are warranted, these modelling and experimental studies indicate that a crystalline repository EBS with bentonite could withstand temperatures up to about 200°C.

5.2. Hydraulic

5.2.x USA

No contribution. US contributors focused on other sections of this report.

5.3. Mechanical

5.3.x USA

The EBS is affected by complex thermal, hydrogeological, mechanical, chemical and biological processes such as heat release due to radionuclide decay, multiphase flow, swelling of buffer materials, radionuclide diffusive transport, waste dissolution, and chemical reactions. A sound understanding of these coupled processes is essential for assessing the safety of the repository. U.S. efforts have led to the development of coupled models and model frameworks to address important mechanical processes in the EBS, including the two mentioned below.

Coupled THMC model for EBS bentonite. Lawrence Berkeley National Laboratory (LBNL) is developing a coupled THMC (Thermal-Hydrological-Mechanical-Chemical) model for long-term EBS bentonite alteration using TOUGHREACT-FLAC3D. The purpose of the coupled THMC model is to quantify bentonite property changes resulting from chemical alteration of smectite and to identify the conditions required to cause significant alteration. Important properties of the bentonite include swelling capacity and sorption capacity. Bentonite has important safety functions including limiting the transport of corrosive reactants to the waste package surface, retarding radionuclide transport, reducing microbial activity, limiting waste package movement, and limiting pressure on the waste package. These properties are affected by corrosion of the waste package and chemical conditions. One of the potential chemical alteration mechanisms is illitization. While illitization is commonly observed in geological formations, experiments do not confirm that this process could be significant in a repository. THMC modelling is expected to provide a means for studying what has been difficult to study in laboratory experiments.

TOUGH-FLAC and TOUGHREACT-FLAC including BBM. LBNL is also developing TOUGH-FLAC, a simulator for multiphase fluid flow and geomechanics, for modelling coupled THM processes in the EBS. Both BBM (Barcelona Basic Model) and BExM (Barcelona Expansive Model) are implemented in TOUGH-FLAC. Coupled THM processes in the EBS in the short term (0 to 1000 years) are important because they may alter the buffer permanently, as indicated in Figure 25. BBM and BExM can model the fundamental behaviour of bentonite. Analysis of the evolution of the DRZ requires a model that includes the EBS and host rock and their interactions. The TOUGH-FLAC model framework with BBM and BExM provides this capability.

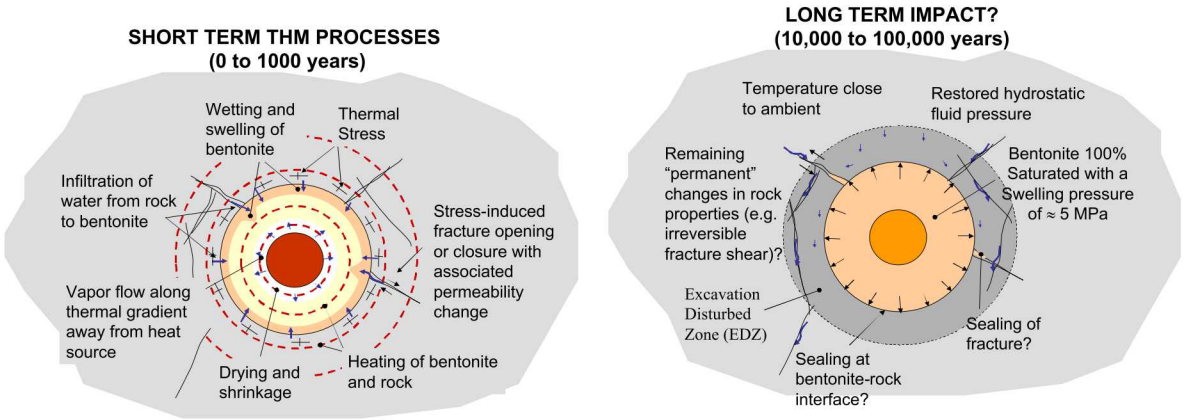

Figure 25. Short-term THM processes in the buffer and potential long-term effects (LBNL).

5.4. Chemical

5.4.x USA

In the U.S. crystalline repository concept, montmorillonite is a major component of the buffer surrounding each waste package. How montmorillonite chemically reacts with radionuclides released from the waste package is expected to have a major effect on radionuclide mobility. In recent years, the U.S. has focused on predictive modelling of radionuclide adsorption to montmorillonite and the chemical effects of montmorillonite on colloids. Three such studies are highlighted here.

Uranium(VI)-montmorillonite surface complexation modelling. US DOE developed a simplified surface complexation model (SCM) to simulate U(VI) adsorption onto Na-montmorillonite in the presence of carbonate over a wide range of chemical solution conditions (Wang et al. 2016). No ternary U(VI)-carbonate adsorption reactions were included. The model indicates the high importance of dissolved carbonate ligands and accurate characterization of electrostatic surface potentials on edge sites. The SCM was used to predict with good accuracy the results of multiple experiments documented in the literature. This work suggests that this modeling approach may be useful for other charge-unbalanced, layered mineral phases.

Plutonium(IV) adsorption and desorption in bentonite. US DOE examined the adsorption and desorption of Pu(IV) to industrial grade FEBEX bentonite (Wang et al. 2015). In batch sorption experiments, after 100 days to reach equilibrium, adsorption was broadly linear over the concentration range of 10^{-7} to 10^{-16} M. For desorption, flow cells were used. The desorption results resembled those of a desorption experiment on SWy-1 montmorillonite. These observations provide quantitative partitioning information for Pu(IV) transport models and suggest the importance of montorillonite in FEBEX bentonite.

Intrinsic colloid stability in the presence of montmorillonite. US DOE studied the behavior of Pu(IV) intrinsic colloids in the presence of montmorillonite at different temperatures (Wang et al. 2015). As illustrated in Figure 26 the experiment employed a dialysis device that kept separate the intrinsic colloids and montmorillonite particles while allowing the aqueous species to mix throughout. The results indicate that the clay particles promoted the dissolution of Pu(IV) intrinsic colloids due to Pu(IV) adsorption to the montmorillonite. Pu(IV) adsorption to montmorillonite was also observed to increase with increasing temperature. This study suggests that while intrinsic Pu(IV) colloids tend to dissolve in the presence of montmorillonite, which limits the mobility of intrinsic colloids, subsequent formation of more stable pseudo-colloids involving montmorillonite could potentially enhance Pu(IV) transport.

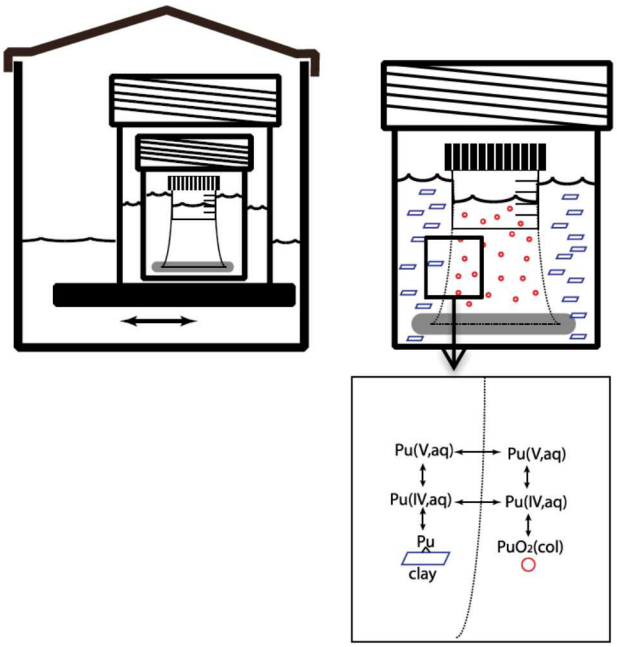

Figure 26. Dialysis membrane experiments on Pu intrinsic colloid stability in the presence of montmorillonite.

5.5. Seal design, buffer / backfill / seal emplacement, voids filling in a DGR in crystalline rocks

5.5.x USA

No contribution. US contributors focused on other sections of this report.

6. Safety assessment

6.1. Assessment context and system description

6.1.x USA

US DOE has completed probabilistic safety assessments in the past 25 years for two deep geologic repositories, one for the disposal of transuranic wastes at the Waste Isolation Pilot Plant (WIPP) in southern New Mexico and one for the disposal of SNF and HLW at the proposed Yucca Mountain repository in Nevada. A probabilistic safety assessment is a key component of the license application. It is needed to provide sufficient confidence that a proposed facility will be in compliance with regulatory safety standards.

Confidence in the ability of a disposal system to meet regulatory safety standards is achieved through a sound understanding of how the engineered and natural barriers will perform over time and how they might be affected by future events. Based on lessons learned from the WIPP and Yucca Mountain experiences, probabilistic safety assessments help build this confidence in three ways: 1) by acknowledging the limits of scientific understanding and accounting for unavoidable and irreducible uncertainties, 2) by identifying how individual components of the system work together to ensure waste isolation, and 3) by quantifying how uncertainties affect overall system performance (Swift and Boyle 2013). Thus, the safety assessment should aim to answer the following three questions (Swift and Boyle 2013):

- Has the analysis appropriately considered the range of scenarios for the future evolution of the repository?
- Does the analysis demonstrate how the components of the system will work together as barriers to isolate the waste under these scenarios?
- How does our uncertainty affect our understanding of the repository's future performance?

In addition to building confidence, probabilistic simulation improves our ability to identify through regression analysis which features, events, and processes (FEPs), or combinations of FEPs, are most important for achieving safety compliance and which have a negligible effect. This information is useful in identifying the strengths and weaknesses in a design and in prioritizing future research.

Safety compliance criteria for geologic nuclear waste repositories in the U.S have generally been site-specific. In principle, the existing U.S. Environmental Protection Agency (US EPA) HLW and SNF radiation protection standards and the U.S. Nuclear Regulatory Commission (US NRC) HLW and SNF regulatory framework originally promulgated in the 1980s (40 CFR 191 and 10 CFR 60, respectively) could apply to a repository in another geologic medium such as crystalline host rock. A specific derivative (40 CFR Part 194) of the EPA standard, 40 CFR 191, currently applies to the WIPP, situated in bedded salt. In 40 CFR 191, the primary indicator of risk to human health is the cumulative release of radionuclides. Its measure is the complementary cumulative distribution function of the cumulative activity release of radionuclides that cross a boundary 5 km from the site 10,000 years after disposal, normalized by (a) EPA-derived limits for specified radionuclides and (b) the mass of radionuclides placed in the repository. However, in 1995 the National Research Council of the National Academies of Science and Engineering recommended using risk to human health as the primary standard for a Yucca Mountain repository. The International Commission on Radiation Protection (ICRP) made a similar recommendation in 1997 (ICRP 1997), and the International Atomic Energy Agency (IAEA) model standard, issued in 2006, uses a dose indicator for deep geologic disposal of radioactive waste (IAEA 2006).

The EPA standard, 40 CFR 197, specifically written for a repository at Yucca Mountain, specifies the hazard indicator measure as the expected (mean) peak dose to a reasonably maximally exposed individual (RMEI) living along the predominant groundwater flow path 18 km from the site. The standard set a limit on expected peak dose rate of 0.15 mSV yr^{-1} (15 mrem yr^{-1}) before 10,000 years and 1 mSv yr^{-1} (100 mrem yr^{-1}) between 10,000 and 1,000,000 years. The latter limit is consistent with the ICRP and IAEA recommendations. The characteristics of the hypothetically exposed individual are those of the RMEI defined in 40 CFR 197. The US EPA and US NRC regulations pertaining to HLW disposal place specific requirements on the major features of PA models intended to demonstrate compliance with regulatory performance objectives. Other details of the regulatory framework,

including screening criteria for potentially relevant FEPs and guidance on inadvertent human intrusion, are assumed to be unchanged from those stated in 40 CFR 197.

6.2. FEPs and scenario analysis related to crystalline rocks

6.2.x USA

A probabilistic safety assessment considers the coupled effects of the features, events, and processes (FEPs) of a proposed disposal system. A full set of reasonable scenarios involving the various FEPs is needed to demonstrate the likely range of repository performance. Scenarios are developed by reviewing complete lists of FEPs and determining which FEPs could potentially affect repository performance.

Each FEP is evaluated against screening criteria provided in U.S. regulations. Specifically, EPA standard 40 CFR 197 states that FEPs that have an annual probability of occurrence lower than 1 in 10^8 during the first 10,000 years after closure may be excluded from the analysis. FEPs that have higher probabilities, but do not significantly change the results of long-term safety assessments, may also be omitted (40 CFR 197.36(a)(1)). In addition, some potentially relevant FEPs are screened from further consideration because they are specifically excluded in the regulatory requirements.

Various programs in the U.S. and other nations have compiled exhaustive lists of FEPs for mined geologic disposal of radioactive wastes. A generic FEPs list was developed by US DOE in 2010 for generic application (Freeze et al. 2010). It was developed from international FEP lists and includes 208 FEPs potentially relevant to a wide range of disposal system alternatives. Revisions to the FEP database is a continuous activity, not only in the U.S. and other countries but also in international NEA projects (Freeze et al. 2017).

Developing relevant scenarios for a safety assessment involves five basic steps (DOE 1996; DOE 2008): 1) identification of a FEPs list; 2) FEPs screening; 3) construction of scenarios from included FEPs for further screening or analysis; 4) selection of scenarios to include in the probabilistic safety assessment; and 5) implementation and analysis of the selected scenarios.

Compared to disposal in other host rock like salt and clay, disposal in crystalline rock relies more heavily on the EBS to contain radionuclides (Wang et al. 2014). A principal function of the geosphere in crystalline rock, therefore, is to provide benign conditions for the EBS. For the U.S. crystalline repository concept, two scenarios are identified for investigation, a glacial scenario and a nominal scenario. Also, because copper and the KBS-3 disposal concept has not been ruled out as an alternative, glacial and nominal scenarios are also applied to the KBS-3 concept.

For steel package and DPC emplacement, generalized or localized corrosion of stainless steel and carbon steel are potentially important processes. The rate and timing of such corrosion depends on the local chemical conditions, which may be affected by various processes occurring in the EBS, such as degradation of waste forms and concrete linings. The resulting corrosion products may provide additional retention capacity through sorption. In the nominal scenario, the buffer remains intact.

The KBS-3 concept relies on the corrosion resistance of copper canisters to contain waste for very long periods. An informative scenario to evaluate in this case is the situation in which one or more copper canisters have an initial defect. SKB implements this scenario by presuming transport through a small defect after the surrounding buffer materials become fully saturated. The defect is then presumed to rapidly expand leading to loss of the waste package containment function. As in the case of emplacement of steel packages and DPCs, the buffer remains intact in the nominal scenario.

The glacial scenario is applied to both the steel waste packages and DPC emplacement concept and to the KBS-3 concept with its copper canisters. This scenario follows the glacial scenario of SKB (SKB 2011, Section 12.2). The retreat of an ice sheet creates transient high infiltration rates, causing large flows of low ionic-strength water to reach repository depths. The low ionic-strength water attacks and erodes the buffer around a portion of the waste packages, exposing the surfaces to higher fluxes of corrosive reactants.

6.3. Modelling (common words)

6.3.1. Modelling of THMC processes in crystalline rock mass and of THMC(B) processes in crystalline rock mass and in EBS

6.3.1.x USA

The foundation of a safety assessment is a computational framework. US DOE is developing a computational framework called Geologic Disposal Safety Assessment (GDSA) Framework. Because US DOE may not perform a new site-specific safety assessment for many years, the long-term goal is to develop a framework that can adapt to, and take advantage of, future advances in computational hardware and process modeling. In line with this goal, the near-term objective is to develop a robust suite of fully functional generic repository reference case applications (1) for future application to potential future candidate sites and (2) for near-term evaluation of the relative importance of FEPs and input parameters on repository performance to inform R&D planning.

Two open-source, freely available, high performance computing (HPC) codes serve as the core of GDSA Framework: PFLOTRAN and Dakota. PFLOTRAN is a massively-parallel thermal-hydrologic-chemical (THC) flow and reactive transport code. Dakota is a versatile probabilistic code used for sampling inputs, sensitivity analysis, and uncertainty quantification.

The flow of data and calculations through GDSA Framework is illustrated in Figure 27. Dakota generates stochastic input for each realization based on parameter uncertainty distributions defined in the input set. Pre-processing software (e.g., CUBIT, dfnWorks, python) generate grids and discrete fracture networks and map spatial properties to grid cells. PFLOTRAN and its coupled process models simulate source term release, EBS evolution, flow and transport through the engineered and natural barriers, and uptake in the biosphere for each realization. Various software (e.g., ParaView, python, VisIt, Dakota) reduce and illustrate the output and evaluate the effects of parameter uncertainty.

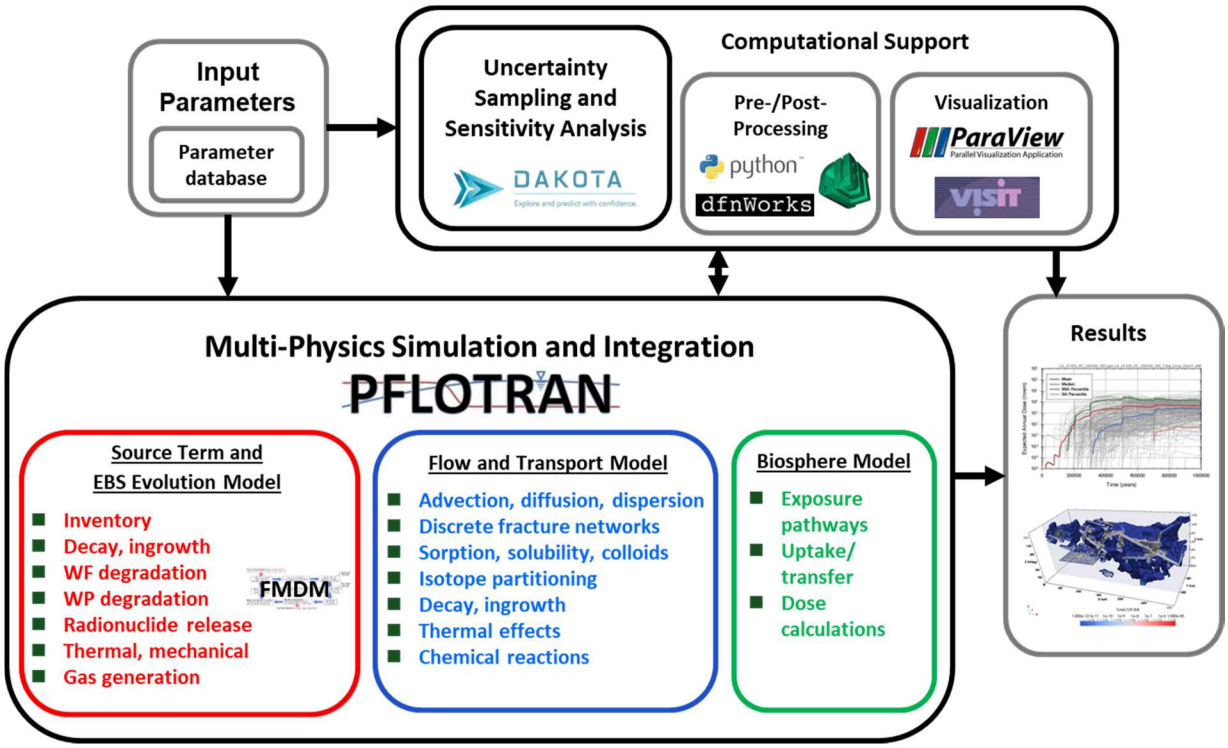

Figure 27. GDSA Framework structure

PFLOTRAN (Hammond et al. 2011a; Lichtner and Hammond 2012) is an open source, reactive multi-phase flow and transport simulator designed to leverage massively-parallel high-performance computing to simulate subsurface earth system processes. PFLOTRAN has been employed on petascale leadership-class US DOE computing resources (e.g., Jaguar at Oak Ridge National Laboratory and Franklin/Hopper at Lawrence Berkeley National Laboratory) to simulate THC processes at the Nevada Test Site (Mills et al. 2007), multi-phase CO_2-H_2O for carbon sequestration (Lu and Lichtner 2007), CO_2 leakage within shallow aquifers (Navarre-Sitchler et al. 2013), and uranium fate and transport at the Hanford 300 Area (Hammond et al. 2007; Hammond et al. 2008; Hammond and Lichtner 2010; Hammond et al. 2011b; Chen et al. 2012; Chen et al. 2013). PFLOTRAN is also under development for future use at the Waste Isolation Pilot Plant (WIPP).

PFLOTRAN solves the non-linear partial differential equations describing non-isothermal multi-phase flow, reactive transport, and geomechanics in porous media. Parallelization is achieved through domain decomposition using the Portable Extensible Toolkit for Scientific Computation (PETSc) (Balay et al. 2013). PETSc provides a flexible interface to data structures and solvers that facilitate the use of parallel computing. PFLOTRAN is written in Fortran 2003/2008 and leverages state-of-the-art Fortran programming (i.e. Fortran classes, pointers to procedures, etc.) to support its object-oriented design. The code provides "factories" within which the developer can integrate a custom set of process models and time integrators for simulating surface and subsurface multi-physics processes. PFLOTRAN employs a single, unified framework for simulating multi-physics processes on both structured and unstructured grid discretizations (i.e. there is no duplication of the code that calculates multi-physics process model functions in support of structured and unstructured discretizations). The code requires a small, select set of third-party libraries (e.g., MPI, PETSc, BLAS/LAPACK, HDF5, Metis/Parmetis). Both the unified structured/unstructured framework and the limited number of third-party libraries greatly facilitate usability for the end user. Additional information can be found at pflotran.org.

PFLOTRAN has been adapted to DGR safety assessment by implementing radioactive decay and ingrowth in all phases including the waste form, isotope partitioning among all phases, an elemental aqueous solubility limit capability, waste form degradation models, a waste package degradation framework, an instantaneous release capability, and a reference biosphere model. Descriptions and demonstrations of these specific capabilities are documented and available at pa.sandia.gov. Application to a generic crystalline rock DGR is described in Section 6.3.2.x.

Further development of GDSA Framework and PFLOTRAN's DGR simulation capabilities will continue for the foreseeable future. Capabilities currently under development include kinetic-based colloidal partitioning and advanced corrosion modelling. Plans for the future include the addition of Pitzer equations for high ionic strength groundwater, coupling of mechanical process models for the buffer and near-field, improved multi-scale and multi-phase transport capabilities, and improved fracture-matrix simulation.

The HPC capabilities of PFLOTRAN and Dakota allow for ever higher fidelity in GDSA Framework applications as more powerful HPC resources become available. Though designed for HPC, PFLOTRAN and GDSA Framework are scalable from supercomputer to laptop. More information on GDSA Framework, including recent papers, presentations, and technical reports, can be found at pa.sandia.org.

6.3.2. Modelling of groundwater flow and radionuclide migration in crystalline rock mass

6.3.2.x USA

US DOE's GDSA Framework has the capability to model fractured rock using either discrete fracture networks (DFNs), networks of two-dimensional planes distributed in a three-dimensional space, or equivalent continuous porous medium (ECPM) representation of DFNs. Flow and transport in both types of models is simulated using PFLOTRAN (see section 6.3.1.x).

Numerical simulation of the crystalline reference case (Mariner et al. 2016) required a method for simulating coupled heat and fluid flow and radionuclide transport in both porous media (bentonite buffer, surface sediments) and fractured rock (the repository host rock). Unless coupled to a porous medium matrix, DFNs cannot be used to simulate heat conduction through the rock matrix, and therefore cannot capture the effects of thermally driven fluid fluxes or be used to couple chemical processes to thermal processes. For these reasons, ECPM were used for performance assessment of the crystalline reference case. When properly defined, an ECPM maintains the flow and transport characteristics of a DFN, allows for uncomplicated placement of porous materials within the model

domain, simulates heat conduction (and solute diffusion) through the matrix of the fractured rock, and allows for fully coupled, transient simulation of reactive transport.

Within GDSA Framework, DFNs are generated with the open-source software dfnWorks developed at Los Alamos National Laboratory (Hyman et al. 2015a; Hyman et al. 2015b) and mapped to ECPM with a Python script (developed at Sandia National Laboratories) called mapDFN (Mariner et al. 2016).

dfnWorks takes as input statistical distributions describing fracture orientation and fracture radii, fracture density (fractures per km^3), parameters relating fracture transmissivity (m^2/s) to fracture radius, and the dimensions of the three-dimensional model domain. It distributes fractures randomly within the space of the model domain and returns only those fractures that belong to a cluster (i.e., it eliminates isolated fractures). For each fracture in a cluster, it returns the coordinates of the fracture center, the unit vector defining the pole normal to the plane of the fracture, and the fracture radius, permeability, and aperture (which is calculated as a function of the fracture transmissivity according to the cubic law).

mapDFN takes as input the output from dfnWorks and parameters describing the desired ECPM model domain and discretization, including the origin and extent of the domain and the length of the grid cells, which are constrained to be cubic. For each grid cell, it calculates anisotropic permeability and fracture porosity by summing the contributions of all fractures intersecting a cell (see Mariner et al. 2016 for more detail). mapDFN assigns all cells in the domain not intersected by fractures user-specified values for matrix permeability and porosity.

A comparison of conservative tracer transport in DFNs and corresponding ECPM generated in this fashion demonstrated reasonably good agreement between the two (Stein et al. 2017). Simulations were run in ~1-km^3 model domain with a 1 Pa/m pressure gradient driving fluid flow. DFNs averaged 1.6 million grid cells. ECPM used a grid cell length of 15 m, and grid cells not intersected by fractures were made inactive. With approximately 32,000 active grid cells, the ECPM ran in a fraction of the time required for DFN simulations. Overall patterns of transport were similar (Figure 28), although in this simulation a false connection in the ECPM is apparent in increased tracer concentrations at the upper left corner of the domain. In general, the DFNs had slightly higher bulk permeability and slightly shorter time of first arrival than their corresponding ECPM.

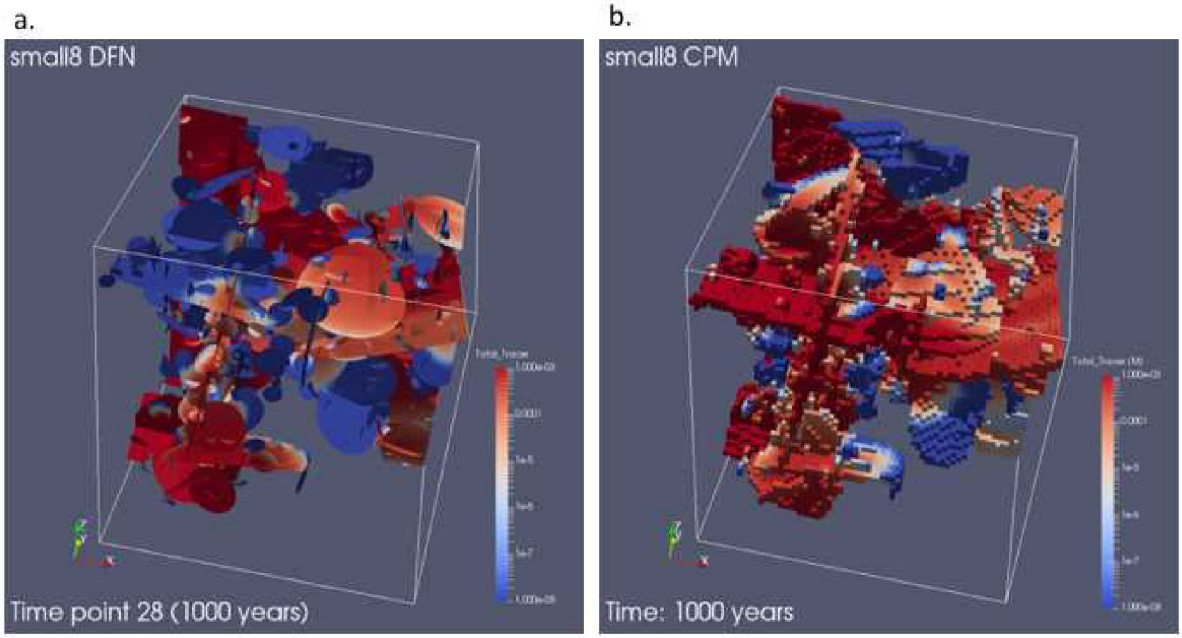

Figure 28. *^{129}I concentration in (a) DFN and (b) ECPM simulations of the same fracture network.*

A set of fracture realizations generated using dfnWorks and converted to ECPM using mapDFN were used in performance assessment of the crystalline reference case (described in Section 3.x.4). Simulated flow and

transport processes included coupled heat and fluid flow, advective and diffusive transport (for simplicity mechanical dispersion was not simulated), sorption using linear distribution coefficients, precipitation and dissolution using solubility limits, and radioactive decay in all phases (aqueous, sorbed, precipitate). A single realization of the model domain, colored by permeability, is shown in Figure 29.

A contour plot of ^{129}I in a different realization is show in Figure 30. The representation of the fractured host rock in this simulation is biased toward greater connectivity than is likely to exist in a sparsely fractured rock selected for nuclear waste disposal. A large fracture density was used to create a system in which flow and transport occurs in the fractures. Having established the capability of simulating flow and transport in a fractured system, we can in the future 1) determine the influence of deterministic features on flow and transport pathways, and 2) determine the probability of a percolating network existing at various length scales given a realistic description of fractured crystalline rock. If a crystalline rock disposal site is selected, site-specific understanding of deterministic features and of the probability of a percolating network existing at the scales of interest will be necessary.

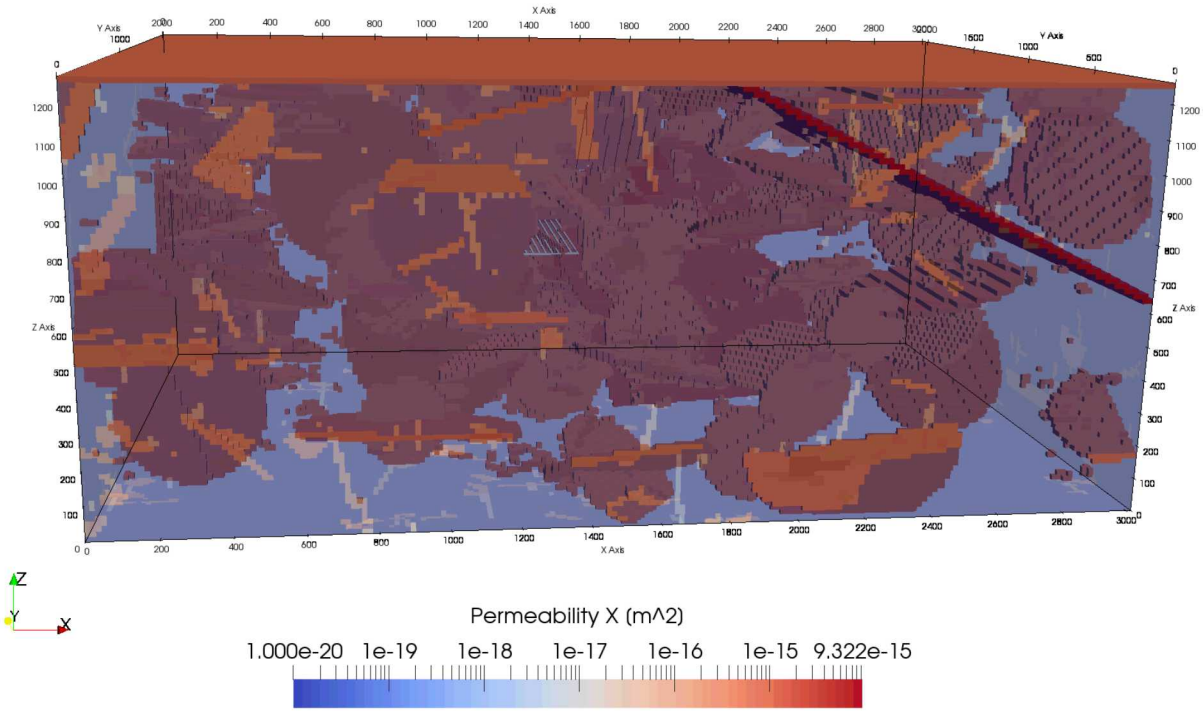

Figure 29. Transparent view of the model domain colored by permeability, showing the largest fractures of a stochastically generated fracture network. Small fractures do not appear in this image because grid cells with permeability less than 5×10^{-16} m^2 were not plotted. The repository (gray) is visible near the center of the model domain.

Future development fracture simulation is likely to take either or both of two paths. The first is development of the ECPM method to improve the comparison to DFNs. False connections in an ECPM result when two or more fractures intersect a grid cell that did not intersect each other in the original DFN. Underrepresentation of the bulk permeability of the domain may result from approximations made in transforming fracture properties into grid cell properties or from differences in path length between ECPM and DFN. Correcting for these problems would enable use of the relatively efficient ECPM method with improved confidence in the results. The second potential development pathway is to couple a porous medium matrix to the DFN, which, although expensive in terms of simulation cost, would enable accurate simulation of fracture-matrix interactions. The ECPM method allows diffusion through the rock matrix to occur, but it does not accurately represent diffusion between fractures and matrix.

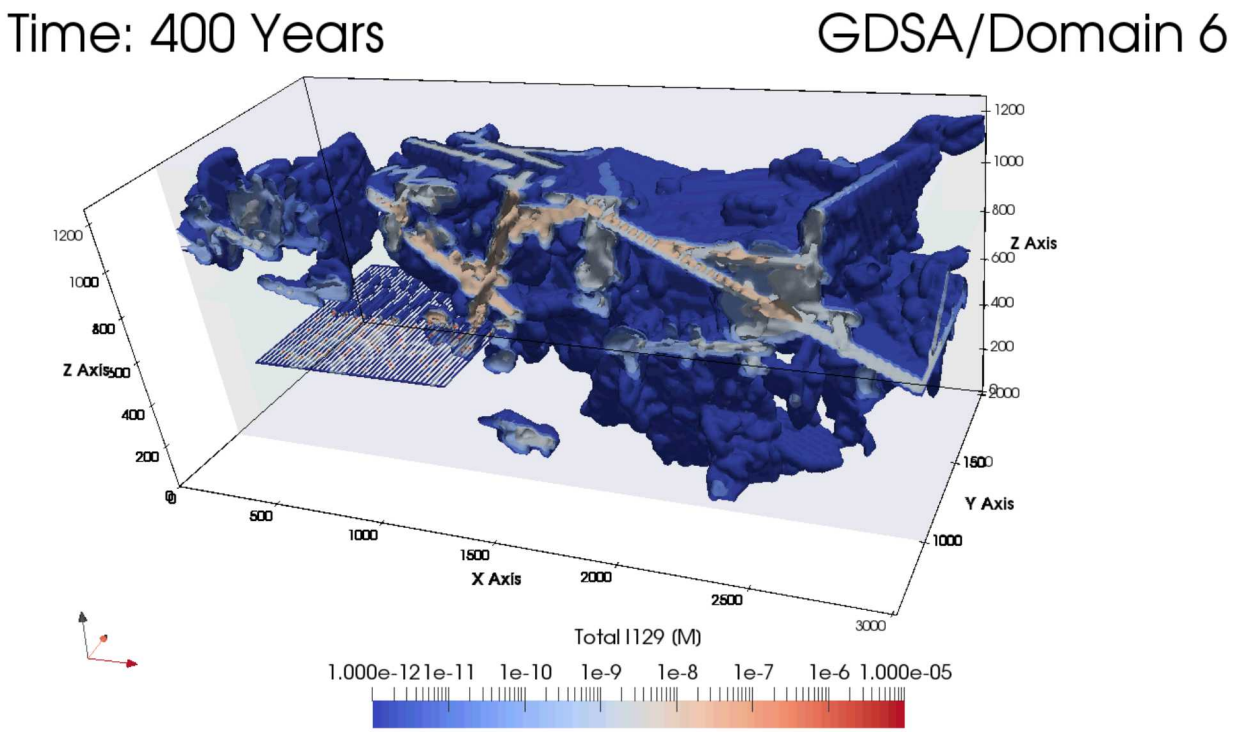

Figure 30. ^{129}I concentration at 400 years in one fracture realization. Concentration is contoured on a log scale at intervals of 10^{-12} mol/L to 10^{-5} mol/L; contours are colored by ^{129}I concentration.

6.3.3. Biosphere transportation models and dose estimation taking into account uncertainty of input data

The realm of the biosphere in DGR safety assessment is the region of human, animal, and plant activity. Wells, aquifers, boreholes, soil, surface water, plants, food chains, air, homes, and environment are all features to be considered in the biosphere. Possible ways for radionuclides to reach the biosphere include disruptive events (e.g., human intrusion), migration to a groundwater well, and migration through the geosphere to the ground surface. Once in the biosphere, numerous FEPs can act to transport, dilute, and concentrate the radionuclides. Each of these biosphere FEPs may affect projected dose rates and exposures to key biota, human and non-human. Dose rates and exposures are key safety metrics of a DGR safety assessment.

Over the past two decades, international efforts have facilitated the advancement biosphere modelling for radioactive waste facilities. In 2016, the IAEA established Working Group 6 (WG6) of its MODARIA II program to advance the BIOMASS example reference biosphere (ERB) methodology developed in IAEA (2003). WG6 is working closely with BIOPROTA (bioprota.org), an international collaboration aimed at improving biosphere modelling for radioactive waste facilities through reduction in key uncertainties in migration and accumulation mechanisms for key radionuclides.

In recent years, biosphere modelling has considered more fully the evolution of climate, landscape, and land use over time. Climate, landscape, and land use may evolve due to global warming, glaciation, societal changes, changing sea levels, erosion, uplift, and other gradual processes that could have a significant probability of occurring at a particular site. These aleatory uncertainties may be included in safety assessment through a set of possible future scenarios.

The primary interest of the Crystalline Club in biosphere modelling is the interface of crystalline rock with the biosphere. An important such interface is a groundwater well. For such a well in crystalline rock to be useful, it must be located in a highly fractured region, either near the ground surface or in a highly-conductive fracture

zone. Other important interfaces are terrestrial outcrops and direct interfaces with surface water and surface water sediments. Each of these interfaces may be affected by climate and landscape changes. For a comprehensive safety assessment, these interfaces and their evolution over time require adequate representation.

Site-specific biosphere models have been developed for several potential or hypothetical DGRs in crystalline rock. The biosphere model for the Forsmark site considers climate change, shoreline displacement, landscape succession, and land use changes (SKB 2014). The safety assessment calculations for that model indicate that the most important path for radionuclides at the Forsmark site is up through the fractured rock to the top layer of the geosphere, facilitated by an upward flux of groundwater. Biosphere modelling for Olkiluoto has similar biosphere ecosystems and evolutionary processes (Posiva 2012). The safety assessment for the Olkiluoto site focusses heavily on land uplift resulting from rebound from the Weichselian maximum 20,000 years ago.

The following subsections describe the status and development of biosphere modelling in the DGR programs of the CRC countries.

6.3.2.x USA

An important metric in repository safety assessment is the annual dose rate to a human from radionuclides that escape the repository. A dose model called Reference Biosphere 1 (RB1) was built into GDSA Framework's PFLOTRAN code to calculate the ingestion dose rate for a person regularly consuming contaminated well water (Mariner et al. 2017, Section 3.2.3).

RB1 includes approximated contributions from "unsupported" radionuclides, as in the model of Olszewska-Wasiolek and Arnold (Olszewska-Wasiolek and Arnold 2011). Unsupported radionuclides are descendants in a decay chain that are not explicitly modelled in the transport calculations due to short half-lives. To include them in the dose calculation, the RB1 model first calculates the aqueous concentrations of the unsupported radionuclides. Total concentrations of unsupported radionuclides in the aquifer are considered to be in secular equilibrium with supporting ancestors. However, aqueous concentrations of unsupported radionuclides further depend on emanation efficiency and adsorption relative to supporting ancestors. If these additional effects are not considered, dose rates can be extremely underestimated, as demonstrated below for ^{222}Rn.

Based on the IAEA (2003) ERB 1A model, the ingestion dose rate $H_{E,i}$ (Sv yr^{-1}) for a supported radionuclide i, such as ^{226}Ra, is calculated using the equation:

$$H_{E,i} = C_{w,i} * I * dcf_i$$

where $C_{w,i}$ is the aqueous concentration (Bq m^{-3}), I is the consumption rate (assumed to be 2 L day^{-1}), and dcf_i is the ingestion dose coefficient (Sv Bq^{-1}). The equivalent equation for an unsupported radionuclide u is (Mariner et al. 2017, Section 3.2.3):

$$H_{E,u} = C_{w,i}\epsilon_u\varphi_u * I * dcf_u$$

where ϵ_u is the sorption enhancement factor and φ_u is the emanation factor. The sorption enhancement factor ϵ_u is the ratio of the retardation factors of the supported and unsupported radionuclides. RB1 calculates ϵ_u from the user-provided adsorption distribution coefficient of the unsupported radionuclide and the retardation factor of the supported radionuclide in the aquifer cells hosting and supplying the well. The emanation factor φ_u is the fraction of the daughter radionuclide concentration unincorporated from solid particles upon generation.

The ^{226}Ra – ^{222}Rn pair is a good example of the potential importance of accounting for emanation efficiency and relative adsorption in unsupported radionuclides. ^{226}Ra has a high retardation factor while its daughter ^{222}Rn has no retardation. In a sandy aquifer, radium has a retardation factor of approximately 5000 (Sheppard and Thibault 1990). If the mean emanation factor of ^{222}Rn is assumed to be 0.4 (as in (Olszewska-Wasiolek and Arnold 2011)), the mean net aqueous enhancement of ^{222}Rn relative to ^{226}Ra is a factor of 2000. Thus, for an aqueous ^{226}Ra concentration of 1 Bq m^{-3}, the corresponding aqueous concentration of ^{222}Rn is 2000 Bq m^{-3}. Although ^{222}Rn has an ingestion dose coefficient that is about 1% of that for ^{226}Ra, its enhanced aqueous concentration causes it to contribute much more to the total annual ingestion dose rate than ^{226}Ra. In this case, ignoring emanation efficiency and relative adsorption of ^{222}Rn would result in an ingestion dose rate from ^{226}Ra and its short-lived descendants that would be underestimated by a factor of 26 (Mariner et al. 2017, Section 3.2.3).

6.4. Uncertainties / confidence in assessment results

6.4.x USA

Performance assessment of the US crystalline reference case has focussed on the effects of spatial variability in the fracture distribution and epistemic uncertainty in select input parameters on radionuclide concentrations at points down gradient of the repository. The uncertainty analysis resulting in Figure 31 was performed to gain understanding of the uncertainty associated with the fracture network and to exercise the uncertainty quantification software (Dakota) in GDSA Framework. This exercise was not intended to address the full range of uncertainty in the problem. In this analysis, only the undisturbed scenario was considered.

As described in Mariner et al. (2016), multiple fracture realizations were generated with dfnWorks using parameters and distributions loosely based on those describing the sparsely fractured metagranite at Forsmark, Sweden (e.g., Joyce et al. 2014). A single fracture realization was chosen for probabilistic analysis of epistemic uncertainty using Dakota.

Dakota is a parallel, object-oriented framework developed by Sandia National Laboratories for uncertainty quantification, sensitivity analysis, parameter estimation, and design optimization (Adams et al. 2014) that is designed to take advantage of high-performance computing. For this application, Latin Hypercube Sampling was used to create multiple realizations of uncertain inputs. Samples of uncertain input parameters were drawn from uniform and log uniform distributions intended to represent likely ranges of parameter values in a crystalline system. Dakota (in conjunction with helper scripts) launches multiple PFLOTRAN simulations and tabulates the desired response functions (maximum radionuclide concentrations at specific locations). Standard output includes sample moments and confidence intervals for each response function, and matrices of simple and rank correlation and partial correlation coefficients relating response functions and uncertain inputs. With additional post-processing, radionuclide breakthrough curves are plotted on horsetail plots. Figure 31 shows how ^{129}I concentration at a point 5 km down-gradient of the repository varies due to fracture realization (a) and due to epistemic uncertainty given a single fracture realization (b).

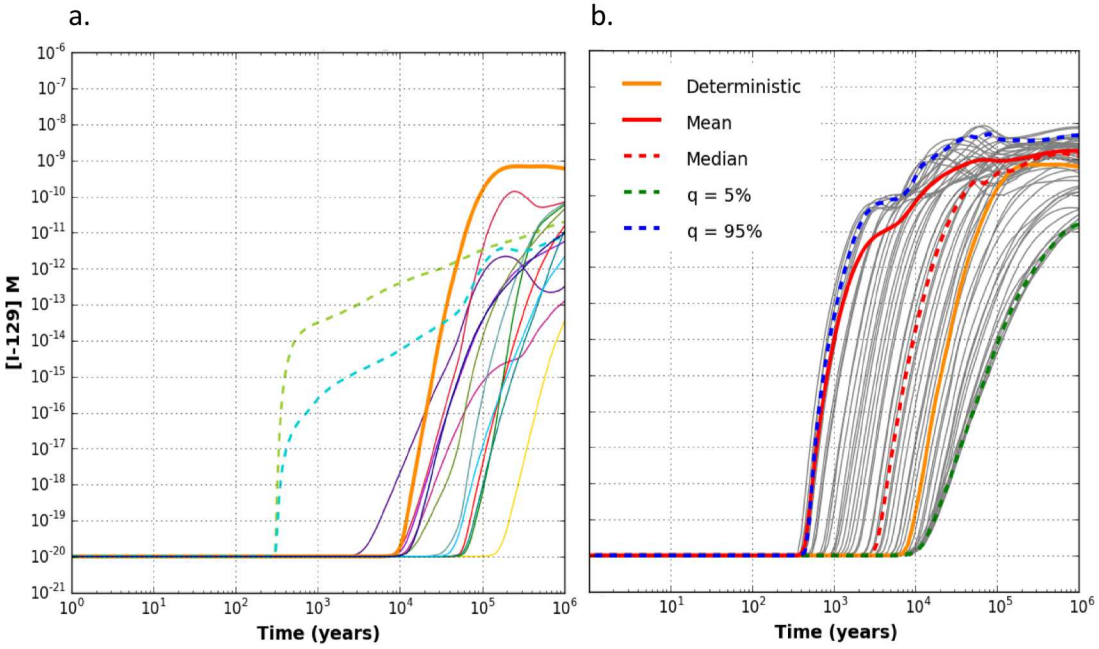

Figure 31. Predicted concentration of ^{129}I versus time for (a) 15 fracture realizations and (b) 50 sampled realizations of a single fracture realization at a point 5-km down-gradient of the repository. The heavy orange line is the same in both plots.

The large uncertainty in both arrival time and maximum concentration due to spatial variability in the fracture distribution reflects variability in location of transport pathways more than it does differences in release from the repository. In the future, combining spatial variability in fracture distribution and epistemic uncertainty in other inputs into a single uncertainty analysis could be desirable. Such an analysis would require re-evaluation of meaningful response functions, and development of a method to incorporate both.

References (Part 1: Pasted)

Adams, B. M. et al. 2017. Dakota, A Multilevel Parallel Object-Oriented Framework for Design Optimization, Parameter Estimation, Uncertainty Quantification, and Sensitivity Analysis: Version 6.6 User's Manual. SAND2014-4633. Updated May 9, 2017.

Altman, S.J., Arnold, B.W., Barnard, R.W., Barr, G.E. Ho, C.K., McKenna, S.A., Eaton, R. R., 1996. Flow calculations for Yucca Mountain groundwater travel time(GWTT-95), SAND96-0819: Albuquerque, New Mexico, Sandia National Laboratories, 170 p.

Barin, I. and Platzki, G. 1995. Thermochemical Data of Pure Substances. 3rd Edition. Two volumes. New York, New York: VCH Publishers.

Berman, R.G. 1988. "Internally-Consistent Thermodynamic Data for Minerals in the System Na2O-K2O-CaO-MgO-FeO-Fe2O3-Al2O3-SiO2-TiO2-CO2." Journal of Petrology, 29, 445-522.

Binnewies, M. and Milke, E. 1999. Thermochemical Data of Elements and Compounds. New York, New York: Wiley-VCH.

BSC (Bechtel SAIC Company) 2007a. Qualification of Thermodynamic Data for Geochemical Modeling of Mineral–Water Interactions in Dilute Systems. ANL-WIS-GS-000003 REV 01. Las Vegas, Nevada: Bechtel SAIC Company. DOC.20070619.0007.

Butscher, Christoph (2012). Steady-State Groundwater Inflow into a Circular Tunnel, Tunnelling and Underground Space Technology, 32 (2012), pp. 158–167.

Carrera, J., Heredia, J., Vomvoris, S., Hufschmied, P., 1990. Modeling of flow on a small fractured monzonitic gneiss block: Selected paper in Hydrogeology of Low Permeability Environments. Int. Assoc. Hydrogeologists Hydrogeol. 2, 115– 167.

Cheshire, M., F.A. Caporuscio, M.S. Rearick, C.F. Jové Colón, and M.K. McCarney, Bentonite evolution at elevated pressures and temperatures: An experimental study for generic nuclear repository designs. American Mineralogist, 2014. 99: p. 1662-1675.

Cox, J.D.; Wagman, D.D.; and Medvedev, V.A., eds. 1989. CODATA Key Values for Thermodynamics. CODATA Series on Thermodynamic Values. New York, New York: Hemisphere Publishing Company.

Dershowitz, B., LaPointe, P., Eiben, T., Wei, L., 1998. Integration of discrete fracture network methods with conventional simulator approaches: Society of Petroleum Engineers Annual Technical Conference and Exhibition, New Orleans, Louisiana (September 27–30), SPE Paper 49069, 9 p.

Dezayes, C., Valley, B., Maqua,E., Syren,G., and Genter, A., 2000. "Natural Fracture System of the Soultz Granite Based on UBI Data in the GPK3 and GPK4 Wells", EC Contract ENK5-2000-00301, BRGM, Synthetic Final Report.

Dolejš D. (2013) Thermodynamics of aqueous species at high temperatures and pressures: Equations of state and transport theory. Reviews in Mineralogy and Geochemistry 76, 35-79.

Dolejš D. and Baker D. R. (2004) Thermodynamic analysis of the system Na2O-K2O-CaO-Al2O3-SiO2-H2O-F2O−1: Stability of fluorine-bearing minerals in felsic igneous suites. Contrib. Mineral. Petrol. 146, 762-778.

Dolejš D. and Wagner T. (2008) Thermodynamic modeling of non-ideal mineral–fluid equilibria in the system Si–Al–Fe–Mg–Ca–Na–K–H–O–Cl at elevated temperatures and pressures: Implications for hydrothermal mass transfer in granitic rocks. Geochim. Cosmochim. Acta 72, 526-553.

ENRESA (2000). Full-scale engineered barriers experiment for a deep geological repository in crystalline host rock FEBEX Project, European Commission: 403.

Gamsjäger, H.; Bugajski, J.; Gajda, T.; Lemire, R.J.; and Preis, W. 2005. Chemical Thermodynamics of Nickel. Chemical Thermodynamics. Volume 6. New York, New York: Elsevier.

García-Siñeriz, J.L., Abós, H., Martínez, V., De la Rosa, C., Mäder, U. and Kober, F., 2016. FEBEX DP: Dismantling of heater 2 at the FEBEX "in situ" test: Description of operations - Arbeitsbericht NAB 16-11, National Cooperative for the Disposal of Radioactive Waste (NAGRA), Wettingen, Switzerland.

Garrels, R.M., and Christ, C.L. 1965 Solutions, Minerals, and Equilibria. Boston, Massachusetts: Jones and Bartlett Publishers

Golder Associates, Inc. (2017). Interactive Discrete Feature Data Analysis, Geometric Modeling and Exploration Simulation, FracMan Manual, April 6, 2017.

Grenthe, I.; Fuger, J.; Konings, R.J.M.; Lemire, R.J.; Muller, A.B.; Nguyen-Trung, C.; and Wanner, H. 1992. Chemical Thermodynamics of Uranium. Chemical Thermodynamics. Volume 1. Amsterdam, The Netherlands: North-Holland Publishing Company.

Guillaumont, R.; Fanghänel, T.; Fuger, J.; Grenthe, I.; Neck, V.; Palmer, D.A.; and Rand, M.H. 2003. Update on the Chemical Thermodynamics of Uranium, Neptunium, Plutonium, Americium and Technetium. Mompean, F.J.; Illemassene, M.; Domenech-Orti, C.; and Ben Said, K., eds. Chemical Thermodynamics. Volume 5. Amsterdam, The Netherlands: Elsevier.

Hadgu, T., Kalinina, E., Lowry, T.S., 2016. Modeling of heat extraction from variably fractured porous media in enhanced geothermal systems. Geothermics 61, 75– 85.

Hammond, G.E., P.C., Lichtner, and R.T., Mills. 2014. Evaluating the Performance of Parallel Subsurface Simulators: An Illustrative Example with PFLOTRAN. J. Water Resources Research. 50, doi:10.1002/2012WR013483.

Hartley, L., Joyce, S., 2013. Approaches and algorithms for groundwater flow modeling in support of site investigations and safety assessment of the Forsmark site Sweden. J. Hydrol. 500, 200–216.

Heinrich C. A., Walshe J. L., and Harrold B. P. (1996) Chemical mass transfer modelling of ore-forming hydrothermal systems: current practice and problems. Ore Geology Reviews 10, 319-338.

Helgeson, H.C. 1969. "Thermodynamics of Hydrothermal Systems at Elevated Temperatures and Pressures." American Journal of Science, 267(6), 729-804.

Helgeson, H.C.; Delany, J.M.; Nesbitt, H.W.; and Bird, D.K. 1978. "Summary and Critique of the Thermodynamic Properties of Rock Forming Minerals." American Journal of Science, 278-A. New Haven, Connecticut: Yale University, Kline Geology Laboratory.

Holland, T.J.B., and Powell, R. 2011. "An Improved and Extended Consistent Thermodynamic Dataset for Phases of Petrological Interest, Involving a New Equation of State for Solids." Journal of Metamorphic Geology, 29, 333-383.

Hsieh, P.A., Neuman, S.P., Stiles, G.K., Simpson, E.S., 1985. Field determination of the three dimensional hydraulic conductivity tensor of anisotropic media, 2, Methodology and application to fractured rocks. Water Resour. Res. 21 (11), 1667–1676.

Huertas, F., Fuentes-Cantillana, J.L., Jullien, F., Rivas, P., Linares, J., Fariña, P., Ghoreychi, M., Jockwer, N., Kickmaier, W., Martínez, M.A., Samper, J., Alonso, E. and Elorza, F.J., 2000. Full-scale engineered barriers experiment for a deep geological repository for high-level radioactive waste in crystalline host rock (FEBEX project): Final report. EUR 19147, European Commission, Brussels.

Hyman, J.D., Karra, S., Makedonska, N., Gable, C.W., Painter, S.L., Viswanathan, H.S., 2015. dfnWorks: A discrete fracture network framework for modeling subsurface flow and transport. Comput. Geosci. 84, 10–19.

Iwatsuki, T., H. Hagiwara, K. Ohmori, T. Munemoto, and H. Onoe. 2015 Hydrochemical disturbances measured in groundwater during the construction and operation of a large-scale underground facility in deep crystalline rock in Japan. J. Environmental Earth Sciences. 74(4): 3041-3057.

Iwatsuki, T.R., R. Furue, H. Mie, S. Ioka, and T. Mizuno. 2005. Hydrochemical baseline condition of groundwater at the Mizunami underground research laboratory (MIU). J. Applied Geochemistry. 20(12): 2283–2302.

Jackson, C.P., Hoch, A.R., Todman, S., 2000. Self-consistency of a heterogenous continuum porous medium representation of a fractured medium. Water Resour. Res. 36 (1), 189–202.

Johnson, J.W.; Oelkers, E.H.; and Helgeson, H.C. 1992. "SUPCRT92: A Software Package for Calculating the Standard Molal Thermodynamic Properties of Minerals, Gases, Aqueous Species, and Reactions from 1 to 5000 Bar and 0 to 1000°C." Computers & Geosciences, 18, (7), 899-947. New York, New York: Pergamon Press.

Kalinina, E, McKenna, S.A., Hadgu, T., Lowry, T.S. (2012a). "Analysis of the Effects of Heterogeneity on Heat Extraction in an EGS Represented with the Continuum Fracture Model", Proceedings, 37-th Workshop on Geothermal Reservoir Engineering, Stanford University, Stanford, California, January 30 - February 1, 2012, SGP-TR-194, 436-445.

Kalinina, E., Hadgu, T., and Wang, Y., 2018. Development and Validation of a Fracture Model for the Granite Rocks at Mizunami Underground Research Laboratory, Japan. Proceedings, ARMA/DFNE 2018, Seattle, WA, June 2018 (in press).

Kalinina, E., McKenna, S.A., Klise, K.A., Hadgu, T., Lowry, T.S., 2014. Applications of fractured continuum model to enhanced geothermal system heat extraction problems. SpringerPlus 3, 110.

Kato,O., Sakagawa, Y., Doi, N., Akaku, K., and Ohkubo, Y., 1999. "Permeable Fractures In The Kakkonda Granite of Well Wd-1b, Japan", Proceedings, Twenty-Fourth Workshop on Geothermal Reservoir Engineering, Stanford University, Stanford, California, January 25-27, 1999.

Klint,E.S., Gravesen, P., Rosenbom,A., Laroche,C., Trenty, L., Lethiez, P., Sanchez, F., Molinelli and Tsakiroglou, C. D., 2004. "Multi-Scale Characterization of Fractured Rocks Used as a Means for the Realistic Simulation of Pollutant Migration Pathways In Contaminated Sites: A Case Study", Water, Air, and Soil Pollution: Focus 4, pp. 201–214.

La Pointe, R.P. (2002). Derivation of parent fracture population statistics from trace length measurements of fractal fracture populations, International Journal of Rock Mechanics & Mining Sciences, 39 (2002), pp. 381–388.

Lemire, R.J., Fuger, J., Nitsche, H., Potter, P., Rand, M.H., Rydberg, J., Spahiu, K., Sullivan, J.C., Ullman, W.J., Vitorge, P., and Wannter, H. 2001. Chemical Thermodynamics of Neptunium and Plutonium. Chemical Thermodynamics. Volume 4. New York, New York: Elsevier.

Lorenz,A., 2007. "Saltwater Intrusion in a Fractured Granite Aquifer", 20th Annual Keck Symposium; pp. 206-211, http://keck.wooster.edu/publications.

Makedonska, N., Hyman, J.D., Karra, S., Painter, S.L., Gable, C.W., Viswanathan, H.S., 2016. Evaluating the effect of internal aperture variability on transport in kilometer scale discrete fracture networks. Adv. Water Resour. 94, 486–497.

Martinez, V., Abós, H. and García-Siñeriz, J.L., 2016. FEBEXe: Final Sensor Data Report (FEBEX "in situ" Experiment) - Arbeitsbericht NAB 16-19, National Cooperative for the Disposal of Radioactive Waste (NAGRA), Wettingen, Switzerland.

Miron G. D., Wagner T., Kulik D. A., and Heinrich C. A. (2016) Internally consistent thermodynamic data for aqueous species in the system Na–K–Al–Si–O–H–Cl. Geochim. Cosmochim. Acta 187, 41-78.

Missana, T. and García-Gutiérrez, M., 2007. Adsorption of bivalent ions (Ca (II), Sr (II) and Co (II)) onto FEBEX bentonite. Physics and Chemistry of the Earth, Parts A/B/C, 32(8): 559-567.

Neuman, S.P., Depner, J.S., 1988. Use of variable-scale pressure test data to estimate the log hydraulic conductivity covariance and dispersivity of fractured granites near Oracle, Arizona. J. Hydrol. 102 (1-4), 475–501.

Olin, A.; Noläng, B.; Öhman, L-O.; Osadchii, E.G.; and Rosén, E. 2005. Chemical Thermodynamics of Selenium. Mompean, F.J.; Perrone, J.; and Illemassène, M., eds. Chemical Thermodynamics. Volume 7. Amsterdam, The Netherlands: Elsevier.

Rard, J.A.; Rand, M.H.; Anderegg, G.; and Wanner, H. 1999. Chemical Thermodynamics of Technetium. Sandino, M.C.A., and Östhols, E., eds. Chemical Thermodynamics 3. Amsterdam, The Netherlands: Elsevier.

Robie, R.A., and Hemingway, B.S. 1995. Thermodynamic Properties of Minerals and Related Substances at 298.15 K and 1 Bar (105 Pascals) Pressure and at Higher Temperatures. Bulletin 2131. Reston, Virginia: U.S. Geological Survey.

Silva, R.J.; Bidoglio, G.; Rand, M.H.; Robouch, P.B.; Wanner, H.; and Puigdomenech, I. 1995. Chemical Thermodynamics of Americium. Chemical Thermodynamics. Volume 2. Amsterdam, The Netherlands: Elsevier.

Sousa, L.M.O., 2007. "Granite Fracture Index to Check Suitability of Granite Outcrops for Quarrying", Engineering Geology, vol. 92 (2007), pp. 146–159.

Tsang, Y.W., Tsang, C.F., Hale, F.V., Dverstop, B., 1996. Tracer transport in a stochastic continuum model of fractured media. Water Resour. Res. 32, 3077– 3092.

Uchida, M., Doe, T., Dershowitz, W., Thomas, A., Wallmann, P., Sawada, A., 1994. Discrete-fracture modeling of the Aspo LPT-2, large-scale pumping and tracer test, SKB International Cooperation report ICR 94–09. Swedish Nuclear Fuel and waste Management Co., Stockholm, Sweden.

Wagman, D.D.; Evans, W.H.; Parker, V.B.; Schumm, R.H.; Halow, I.; Bailey, S.M.; Churney, K.L.; and Nuttall, R.L. 1982. "The NBS Tables of Chemical Thermodynamic Properties, Selected Values for Inorganic and C1 and C2 Organic Substances in SI Units." Journal of Physical and Chemical Reference Data, 11, (Supplement No. 2), 2-276 - 2-282. Washington, D.C.: American Chemical Society.

Wagman, D.D.; Evans, W.H.; Parker, V.B.; Schumm, R.H.; Halow, I.; Bailey, S.M.; Churney, K.L.; and Nuttall, R.L. 1989. "Erratum: The NBS Tables of Chemical Thermodynamic Properties, Selected Values for Inorganic and C1 and C2 Organic Substances in SI Units." Journal of Physical and Chemical Reference Data, 18, (4), 2-276 - 2-282, 1807-1812. Washington, D.C.: American Chemical Society.

Wang, Y., Hadgu, T., Kalinina, E., Jerden, J., Gattu, V. K., Ebert, W., Viswanathan, H., hyman, J., Karra, S., Knapp, N., Makedonska, N, Reimus, P., Telfeyan, K., Fox, P. M., Nico, P. S., Zavarin, M., Balboni, E., and Atkins-Duffin, C., 2017. Evaluation of Spent Fuel Disposition in Crystalline Rocks: FY17 Progress Report, SFWD-SFWST-2017-000007.

Younes, A., Engelder,T., and Bosworth, W., 1998. "Fracture Distribution in Faulted Basement Blocks: Gulf of Suez, Egypt", Geological Society, London, Special Publications, January 1, 1998, vol. 127, pp. 167-190.

Zak,J., Verner,K., Klomınsky,J., Chlupacova,M., 2009. ''Granite tectonics Revisited: Insights from Comparison of K-Feldspar Shape-Fabric, Anisotropy of Magnetic Susceptibility (AMS), and Brittle Fractures in the Jizera Granite, Bohemian Massif", International Journal of Earth Sciences (Geol Rundsch), vol. 98, pp. 949–967.

Zhang, H.H. Einstein and Dershowitz, W.S. (2002). Stereological relationship between trace length and size distribution of elliptical discontinuities, Geotechnique, 52/6 (2002), pp. 419-433.
Zhang, X., Sanderson, D.J., 2002. Numerical Modelling and Analysis of Fluid Flow and deformation of Fractured Rock Masses. Elsevier, London. 300pp.
Zheng, L. J. Rutqvist, H. Xu, K. Kim, M. Voltolini, and X. Cao (2017). Investigation of Coupled Processes and Impact of High Temperature Limits in Argillite Rock: FY17 Progress. SFWD-SFWST-2017-000040. Lawrence Berkeley National Laboratory, Berkeley, California.

References (Part 2: From EndNote)

Adams, B. M., M. S. Ebeida, M. S. Eldred, G. Geraci and J. D. Jakeman (2014). Dakota, A Multilevel Parallel Object-Oriented Framework for Design Optimization, Parameter Estimation, Uncertainty Quantification, and Sensitivity Analysis: Version 6.7 User's Manual. SAND2014-4633. Sandia National Laboratories, Albuquerque, New Mexico.
Balay, S., J. Brown, K. Buschelman, V. Eijkhout, W. D. Gropp, D. Kaushik, M. G. Knepley, L. Curfman McInnes, B. F. Smith and H. Zhang (2013). PETSc Users Manual. ANL-95/11 – Revision 3.4. Argonne National Laboratory, Argonne, Illinois.
Bonano, E. J., E. A. Kalinina and P. N. Swift (2018). "The Need for Integrating the Back End of the Nuclear Fuel Cycle in the United States of America," *MRS Advances*, **3**(19):991-1003.
Caporuscio, F. A., M. C. Cheshire and M. McCarney (2012). "Bentonite Clay Evolution at Elevated Pressures and Temperatures: An experimental study for generic nuclear repositories," 2012 American Geophysical Union (AGU) Fall Meeting, San Francisco, California.
Carter, J. T., A. J. Luptak, J. Gastelum, C. Stockman and A. Miller (2013). Fuel Cycle Potential Waste Inventory for Disposition. FCRD-USED-2010-000031 Rev 6. Savannah River National Laboratory, Aiken, South Carolina.
Chen, X., G. Hammond, C. Murray, M. Rockhold, V. Vermeul and J. Zachara (2013). "Applications of ensemble-based data assimilation techniques for aquifer characterization using tracer data at Hanford 300 area," *Water Resources Research*, **49**:7064-7076.
Chen, X., H. Murakami, M. Hahn, G. E. Hammond, M. L. Rockhold, J. M. Zachara and Y. Rubin (2012). "Three-Dimensional Bayesian Geostatistical Aquifer Characterization at the Hanford 300 Area using Tracer Test Data," *Water Resources Research*, **48**.
Cheshire, M. C., F. A. Caporuscio, C. F. Jové Colón and M. K. McCarney (2013). "Alteration of clinoptilolite into high-silica analcime within a bentonite barrier system under used nuclear fuel repository conditions," International High-Level Radioactive Waste Management (2013 IHLRWM) Conference, Albuquerque, New Mexico.
Cheshire, M. C., F. A. Caporuscio, M. S. Rearick, C. Jove-Colon and M. K. McCarney (2014). "Bentonite evolution at elevated pressures and temperatures: An experimental study for generic nuclear repository designs," *American Mineralogist*, **99**(8-9):1662-1675.
Cho, W. J., J. S. Kim, C. Lee and H. J. Choi (2013). "Gas permeability in the excavation damaged zone at KURT," *Engineering Geology*, **164**:222-229.
DOE (1996). Title 40 CFR Part 191. U.S. Department of Energy, Carlsbad, New Mexico.
DOE (2008). Yucca Mountain Repository Safety Analysis Report. Office of Civilian Radioactive Waste Management, U.S. Department of Energy, Las Vegas, Nevada.
Follin, S., L. Hartley, I. Rhen, P. Jackson, S. Joyce, D. Roberts and B. Swift (2014). "A methodology to constrain the parameters of a hydrogeological discrete fracture network model for sparsely fractured crystalline rock, exemplified by data from the proposed high-level nuclear waste repository site at Forsmark, Sweden," *Hydrogeology Journal*, **22**(2):313-331.

Freeze, G., D. Sevougian, M. Gross, K. Kuhlman, J. Wolf and D. Buhmann (2017). "FEP Catalogue, Database, and Knowledge Archive," 8th US/German Workshop on Salt Repository Research, Design, and Operation, Middelburg, The Netherlands, September 5-7, 2017.

Freeze, G. A., P. E. Mariner, J. E. Houseworth and J. C. Cunnane (2010). Used Fuel Disposition Campaign Features, Events, and Processes (FEPs): FY10 Progress Report. Sandia National Laboratories, Albuquerque, New Mexico.

García-Siñeriz, J. L., H. Abós, V. Martínez, C. De la Rosa, U. Mäder and F. Kober (2016). FEBEX DP: Dismantling of heater 2 at the FEBEX "in situ" test: Description of operations - Arbeitsbericht NAB 16-11. National Cooperative for the Disposal of Radioactive Waste (NAGRA). Wettingen, Switzerland. **NAB 16-11:** 1-136.

Gunter, T. C. and P. K. Nair (2016). Research & Development Program for the Used Nuclear Fuel and High-Level Radioactive Waste Disposition in the United States. Chapter 24 of International Approaches for Deep Geological Disposal of Nuclear Waste: Geological Challenges in Radioactive Waste Isolation, Fifth Worldwide Review (eds., B. Faybishenko, J. Birkholzer, D. Sassani, and P. Swift). Prepared for U.S. Department of Energy. LBNL-1006984. Lawrence Berkeley National Laboratory (LBNL) and Sandia National Laboratories (SNL),

Hammond, G., P. Lichtner and C. Lu (2007). "Subsurface multiphase flow and multicomponent reactive transport modeling using high performance computing," *Journal of Physics: Conference Series 78*:1-10.

Hammond, G. E. and P. Lichtner (2010). "Field-scale modeling for the natural attenuation of uranium at the Hanford 300 area using high performance computing," *Water Resources Research*, **46**.

Hammond, G. E., P. C. Lichtner, C. Lu and R. T. Mills (2011a). "PFLOTRAN: Reactive Flow and Transport Code for Use on Laptops to Leadership-Class Supercomputers." Groundwater Reactive Transport Models. F. Zhang, G. T. Yeh and J. Parker. Bentham Science Publishers.

Hammond, G. E., P. C. Lichtner, R. T. Mills and C. Lu (2008). "Toward petascale computing in geosciences: application to the Hanford 300 Area," *Journal of Physics Conference Series*, **125**:12051-12051.

Hammond, G. E., P. C. Lichtner and M. L. Rockhold (2011b). "Stochastic simulation of uranium migration at the Hanford 300 Area," *Journal of Contaminant Hydrology*, **120-121**:115-128.

Huertas, F., J. L. Fuentes-Cantillana, F. Jullien, P. Rivas, J. Linares, P. Fariña, M. Ghoreychi, N. Jockwer, W. Kickmaier, M. A. Martínez, J. Samper, E. Alonso and F. J. Elorza (2000). Full-scale engineered barriers experiment for a deep geological repository for high-level radioactive waste in crystalline host rock (FEBEX project): Final report. EUR 19147. European Commission, Brussels.

Hyman, J. D., S. Karra, N. Makedonska, C. W. Gable, S. L. Painter and H. S. Viswanathan (2015a). "dfnWorks: A discrete fracture network framework for modeling subsurface flow and transport," *Computers & Geoscience*, **84**:10-19.

Hyman, J. D., S. L. Painter, H. Viswanathan, N. Makedonska and S. Karra (2015b). "Influence of injection mode on transport properties in kilometer-scale three-dimensional discrete fracture networks," *Water Resources Research*, **51**(9):7289-7308.

IAEA (2003). "Reference Biospheres" for Solid Radioactive Waste Disposal. International Atomic Energy Agency, Vienna, Austria.

IAEA (2006). Geological Disposal of Radioactive Waste. International Atomic Energy Agency, Vienna, Austria.

ICRP (1997). "ICRP Publication 77: Radiological Protection Policy for the Disposal of Radioactive Waste," *Annals of the ICRP*, **27**(Supplement).

Jové Colón, C. F., J. A. Greathouse, S. Teich-McGoldrick, R. T. Cygan, T. Hadgu, J. E. Bean, M. J. Martinez, P. L. Hopkins, J. G. Arguello, F. D. Hansen, F. A. Caporuscio and M. Cheshire (2012). Evaluation of Generic EBS Design Concepts and Process Models: Implications to EBS Design Optimization. FCRD-USED-2012-000140. U.S. Department of Energy, Washington D.C.

Joyce, S., L. Hartley, D. Applegate, J. Hoek and P. Jackson (2014). "Multi-scale groundwater flow modeling during temperate climate conditions for the safety assessment of the proposed high-level nuclear waste repository site at Forsmark, Sweden," *Hydrogeology Journal*, **22**(6):1233-1249.

Lichtner, P. C. and G. E. Hammond (2012). Quick Reference Guide: PFLOTRAN 2.0 (LA-CC-09-047) Multiphase-Multicomponent-Multiscale Massively Parallel Reactive Transport Code. LA-UR-06-7048. December 8, 2012. Los Alamos National Laboratory, Los Alamos, New Mexico.

Liu, H. H., J. Houseworth, J. Rutqvist, L. Zheng, D. Asahina, L. Li, V. Vilarrasa, F. Chen, S. Nakagawa, S. Finsterle, C. Doughty, T. Kneafsey and J. Birkholzer (2013). Report on THMC modeling of the near field evolution of a generic clay repository: Model validation and demonstration. FCRD-UFD-2013-0000244. Lawrence Berkeley National Laboratory, Berkeley, California.

Lu, C. and P. C. Lichtner (2007). "High resolution numerical investigation on the effect of convective instability on long term CO_2 storage in saline aquifers," *Journal of Physics Conference Series*, **78**:U320-U325.

Marcinowski, F. (2010). Overview of DOE's Spent Nuclear Fuel and High-Level Waste. Presentation to the Blue Ribbon Commission on America's Nuclear Future, March 25, 2010, Washington, DC.

Mariner, P. E., J. H. Lee, E. L. Hardin, F. D. Hansen, G. A. Freeze, A. S. Lord, B. Goldstein and R. H. Price (2011). Granite Disposal of U.S. High-Level Radioactive Waste. SAND2011-6203. Sandia National Laboratories, Albuquerque, New Mexico

Mariner, P. E., E. R. Stein, J. M. Frederick, S. D. Sevougian and G. E. Hammond (2017). Advances in Geologic Disposal System Modeling and Shale Reference Cases. SFWD-SFWST-2017-000044, SAND2017-10304 R. Sandia National Laboratories, Albuquerque, New Mexico.

Mariner, P. E., E. R. Stein, J. M. Frederick, S. D. Sevougian, G. E. Hammond and D. G. Fascitelli (2016). Advances in Geologic Disposal System Modeling and Application to Crystalline Rock. FCRD-UFD-2016-000440, SAND2016-9610 R. Sandia National Laboratories, Albuquerque, New Mexico.

Martinez, V., H. Abós and J. L. García-Siñeriz (2016). FEBEXe: Final Sensor Data Report (FEBEX "in situ" Experiment) - Arbeitsbericht NAB 16-19. National Cooperative for the Disposal of Radioactive Waste (NAGRA). Wettingen, Switzerland. **NAB 16-19:** 1-250.

Martino, J. B. and N. A. Chandler (2004). "Excavation-induced damage studies at the Underground Research Laboratory," *International Journal of Rock Mechanics and Mining Sciences*, **41**(8):1413-1426.

Mills, R., C. Lu, P. C. Lichtner and G. Hammond (2007). "Simulating subsurface flow and transport on ultrascale computers using PFLOTRAN," 3rd Annual Scientific Discovery through Advanced Computing Conference (SciDAC 2007), BostonJournal of Physics Conference Series, U387-U393.

Missana, T. and M. García-Gutiérrez (2007). "Adsorption of bivalent ions (Ca (II), Sr (II) and Co (II)) onto FEBEX bentonite," *Physics and Chemistry of the Earth, Parts A/B/C*, **32**(8):559-567.

Navarre-Sitchler, A., R. M. Maxwell, E. R. Siirila, G. E. Hammond and P. C. Lichtner (2013). "Elucidating geochemical response of shallow heterogeneous aquifers to CO_2 leakage using high-performance computing: implications for monitoring CO_2 sequestration," *Advances in Water Resources*, **53**:44-55.

Olszewska-Wasiolek, M. A. and B. W. Arnold (2011). "Radioactive Disequilibria in the Saturated Zone Transport Model and the Biosphere Model for the Yucca Mountain Repository — The Case of Radon-222," International High-Level Radioactive Waste Management Conference, Albuquerque, New Mexico, 767-772.

Patrick, W. C. (1986). Spent-Fuel Test - Climax: An Evaluation of the Technical Feasibility of Geologic Storage of Spent Nuclear Fuel in Granite. Lawrence Livermore National Laboratory, Livermore, California.

Posiva (2012). Olkiluoto Biosphere Description 2012. POSIVA 2012-06. Posiva Oy, Olkiluoto, Finland.

Pusch, R., P. Bluemling and L. Johnson (2003). "Performance of strongly compressed MX-80 pellets under repository-like conditions," *Applied Clay Science*, **23**(1-4):239-244.

Pusch, R., J. Kasbohm and H. T. M. Thao (2010). "Chemical stability of montmorillonite buffer clay under repository-like conditions-A synthesis of relevant experimental data," *Applied Clay Science*, **47**(1-2):113-119.

Schild, M., S. Siegesmund, A. Vollbrecht and M. Mazurek (2001). "Characterization of granite matrix porosity and pore-space geometry by in situ and laboratory methods," *Geophysical Journal International*, **146**(1):111-125.

Sheppard, M. I. and D. H. Thibault (1990). "Default soil solid/liquid partition coefficients, Kds, for four major soil types: a compendium," *Health Physics*, **59**(4):471-482.

SKB (2007). Geology Forsmark. R-07-45. Svensk Karnbranslehantering AB, Stockholm, Sweden.

SKB (2008). Bedrock hydrogeology Forsmark. R-08-45. Svensk Karnbranslehantering AB, Stockholm, Sweden.

SKB (2011). Long-term safety for the final repository for spent nuclear fuel at Forsmark. Svensk Kärnbränslehantering AB, Stockolm, Sweden.

SKB (2014). Biosphere synthesis report for the safety assessment SR-PSU. TR-14-06. Svensk Kärnbränslehantering AB, Stockholm, Sweden.

SNL (1993). Initial Performance Assessment of the Disposal of Spent Nuclear Fuel and High-Level Waste Stored at Idaho National Engineering Laboratory. R. P. Rechard. Sandia National Laboratories, Albuquerque, New Mexico.

Soler, J. M., J. Landa, V. Havlova, Y. Tachi, T. Ebina, P. Sardini, M. Siitari-Kauppi, J. Eikenberg and A. J. Martin (2015). "Comparative modeling of an in situ diffusion experiment in granite at the Grimsel Test Site," *Journal of Contaminant Hydrology*, **179**:89-101.

Stein, E. R., J. M. Frederick, G. E. Hammond, K. L. Kuhlman, P. E. Mariner and S. D. Sevougian (2017). "Modeling Coupled Reactive Flow Processes in Fractured Crystalline Rock," 16th International High-Level Radioactive Waste Management Conference, Charlotte, North Carolina, April 9-13, American Nuclear Society.

Stone, D., D. C. Kamineni, A. Brown and R. Everitt (1989). "A comparison of fracture styles in 2 granite bodies of the Superior Province," *Canadian Journal of Earth Sciences*, **26**(2):387-403.

Swift, P. N. and W. J. Boyle (2013). "Using safety assessment techniques to build confidence in repository performance: The United States experience," The Safety Case for Deep Geological Disposal of Radioactive Waste: 2013 State of the Art, Paris, France, October 7-9, 2013, Nuclear Energy Agency, pp. 29-36.

Wang, Y., T. Hadgu, E. A. Kalinina, J. Jerden, J. M. Copple, T. Cruse, W. Ebert, E. Buck, R. Eittman, R. Tinnacher, C. Tournassat, J. Davis, H. Viswanathan, S. Chu, T. Dittrich, F. Hyman, S. Karra, N. Makedonska, P. Reimus, M. Zavarin and C. Joseph (2016). Used Fuel Disposition in Crystalline Rocks: FY16 Progress Report. FCRD-UFD-2016-000076, SAND2015-9297 R. Sandia National Laboratories, Albuquerque, New Mexico.

Wang, Y., T. Hadgu, E. Matteo, J. N. Kruichak, M. M. Mills, R. Tinnacher, J. Davis, H. S. Viswanathan, S. Chu, T. Dittrich, F. Hyman, S. Karra, N. Makedonska, P. Reimus, M. Zavarin, P. Zhao, C. Joseph, J. B. Begg, Z. Dai, A. B. Kersting, J. Jerden, J. M. Copple, T. Cruse and W. Ebert (2015). Used Fuel Disposal in Crystalline Rocks: FY15 Progress Report. FCRD-UFD-2015-000125. Sandia National Laboratories, Albuquerque, New Mexico.

Wang, Y., E. Matteo, J. Rutqvist, J. Davis, L. Zheng, J. Houseworth, J. Birkholzer, T. Dittrich, C. W. Gable, S. Karra, N. Makedonska, S. Chu, D. Harp, S. L. Painter, P. Reimus, F. V. Perry, P. Zhao, J. B. Begg, M. Zavarin, S. J. Tumey, Z. R. Dai, A. B. Kersting, J. Jerden, K. E. Frey, J. M. Copple and W. Ebert (2014). Used Fuel Disposal in Crystalline Rocks: Status and FY14 Progress. FCRD-UFD-2014-000060, SAND2014-17992 R. Sandia National Laboratories, Albuquerque, New Mexico.

Wang, Y., A. Miller, E. Matteo, P. Reimus, M. Ding, T. Dittrich, L. Zheng, J. Houseworth, P. Zhao, A. Kersting, A. Dai and M. Zavarin (2013). Experimental and Modeling Investigation of Radionuclide Interaction and Transport in Representative Geologic Media. FCRD-UFD-2013-000314. U.S. Department of Energy, Washington D.C.

Wersin, P., L. H. Johnson and I. G. McKinley (2007). "Performance of the bentonite barrier at temperatures beyond 100 degrees C: A critical review," *Physics and Chemistry of the Earth*, **32**(8-14):780-788.

Zheng, L., J. Houseworth, C. Steefel, J. Rutqvist and J. Birkholzer (2014). Investigation of Coupled Processes and Impact of High Temperature Limits in Argillite Rock. FCRD-UFD-2014-000493. U.S. Department of Energy, Washington D.C.